Palaeogeography, Palaeoclimatology, Palaeoecology 617 (2023) 111499

Contents lists available at ScienceDirect

Palaeogeography, Palaeoclimatology, Palaeoecology

journal homepage: www.elsevier.com/locate/palaeo

Late Holocene Vistula River floods recorded in grain size distributions and diatom assemblages of marine sediments of the Gulf of Gdańsk (Baltic Sea)

Marta Szcześniak [a], Mikołaj Kokociński [b], Robert Jagodziński [a], Krzysztof Pleskot [a], Marek Zajączkowski [c], Witold Szczuciński [a,*]

[a] Geohazards Research Unit, Institute of Geology, Adam Mickiewicz University, Poznań, Bogumiła Krygowskiego 12, 61-680 Poznań, Poland
[b] Department of Hydrobiology, Adam Mickiewicz University, Poznań, Uniwersytetu Poznańskiego 6, 61-614 Poznań, Poland
[c] Institute of Oceanology, Polish Academy of Sciences, Powstańców Warszawy 55, 81-712 Sopot, Poland

ARTICLE INFO

Editor: M Elliot

Keywords:
Continental shelf
Diatoms
Grain size
River floods
Late Holocene
Baltic Sea

ABSTRACT

During the large flood of the Vistula River in 2010, the riverine brackish water surface plume extended up to 70 km into the Gulf of Gdańsk (Baltic Sea), leaving a thin layer of medium-grained sand deposits. It inspired a search for palaeoflood records in marine sediments. Thus, we aimed to identify the most useful flood indicators and apply them to reveal palaeoflood records in sediment cores from the Gulf of Gdańsk. The study is based on analyses of surface samples, collected during and one year after the 2010 flood, and two long sediment cores, which were subjected to high-resolution grain size, diatom, and geochemical analyses, while chronology was based on the combined AMS ^{14}C, ^{210}Pb and ^{137}Cs dating. It was found that, in a water depth of less than 30 m, modern large flood deposits were not preserved after a year. Sediment cores retrieved from greater water depths (over 60 m) were composed of sandy mud, and most of the 1 cm thick sediment samples were characterized by unimodal grain size distribution. However, some of the samples were bimodal, with the additional mode in fine-grained fractions, which is interpreted to be the result of direct deposition from riverine flood surface water plume. The diatom assemblages revealed a moderate downcore variability, except for the intervals characterized by bimodal grain size distributions. They contained elevated amounts of benthic oligohalobous (freshwater) and decreased euhalobous and mesohalobous taxa, supporting the likely interpretation of these layers as deposited during river flood events. During the last c. 4 ka, a dozen major flood events were identified. However, their application to flood climate reconstruction is challenging because of relatively frequent and partly unknown changes in major river mouth positions in the past. We suggest that thin deposits of major floods left on the seafloor and subjected to further mixing maybe still recognized using a combination of high-resolution grain size distribution and diatom analyses supplemented by a good understanding of the depositional system history.

1. Introduction

In the global context, the areas of large river deltas are particularly susceptible to dynamic environmental changes, including floods, storms, and increasing sea level. They also witness problems of socio-economical nature, e.g., shortage of drinking water or progressing degradation of the deltas area (Milliman, 1997; Overeem and Syvitski, 2009; Syvitski et al., 2009; Anthony, 2015; Smith et al., 2015; Voosen, 2019). These changes are of critical importance since the coastal zones and large river deltas combined are inhabited by circa 30% of the world's population (Douglas, 2001; Douglas and Peltier, 2002; Overeem and Syvitski, 2009). Some of the processes affecting the deltas are related to human activity. In contrast, the others are inherently natural phenomena, and their long-term frequency could be assessed only by studies of sedimentary records.

Sediment discharge to the seas and oceans is controlled by many factors, i.e., basin relief, evaporation, precipitation, vegetation (Milliman and Syvitski, 1992), and human activity. Whereas at the zone of the river mouths also shelf geometry, tides, waves and coastal sediment transport can play a significant role (Nittrouer and Wright, 1994). Moreover, high-energy events, including floods (Wheatcroft and Borgeld, 2000), storms (Ogston et al., 2000), hurricanes (Keen et al., 2004) or tsunamis (Sakuna et al., 2012), have often been reported to alter the depositional conditions on the continental shelf. These events may be

* Corresponding author.
E-mail address: witek@amu.edu.pl (W. Szczuciński).

https://doi.org/10.1016/j.palaeo.2023.111499
Received 30 June 2022; Received in revised form 22 February 2023; Accepted 6 March 2023
Available online 10 March 2023

recorded in marine sediments and have a significant impact on the coastal ecosystems, e.g. through a rapid discharge of the vast amount of terrestrial organic matter and sediments.

The Vistula River is the largest river in the Baltic Sea catchment and has undergone numerous transformations in the past. They include several alterations of the Vistula River mouth location, development of the inner Vistula Delta plain (Żuławy Wiślane), and artificial formation of the lower river course and mouth – the Vistula Cross-Cut (Przekop Wisły) in 1895 (Fig. 1). The latter resulted in decreased accumulation within the inner delta plain and an establishment of a new sedimentary depocentre in the Gulf of Gdańsk. Although, many studies on various aspects of environmental changes recorded in the Gulf of Gdańsk sediments have been carried out (e.g., Sternbeck et al., 2000; Uścinowicz, 2003; Dippner and Voss, 2004; Witak, 2010; Szymczak-Żyła and Kowalewska, 2009; Szymczak-Żyła et al., 2017, 2019; Uścinowicz et al., 2022), and recent flood (e.g., the largest during the last 130 years Vistula River flood in the 2010) or storm events (Zajączkowski et al., 2010; Moskalewicz et al., 2020; Leszczyńska et al., 2022) proved the potential importance of these processes in the Gulf of Gdańsk, the studies focused on long-term sedimentary flood records are missing, so far. These geological records are potentially important in the context of ongoing climate change and related variations in the frequency and magnitude of extreme events, as they may provide the testing ground for climate models.

There are several proxies of the flood record in marine sediments established for rivers with large sediment discharge, often leaving a clear flood layer within continental shelf deposits, e.g., increased silt fraction content or increased terrigenous organic carbon content in the event layer sediments (Wheatcroft et al., 1996; Sommerfield and Nittrouer, 1999). They are based on two flood-induced changes: i) increased river sediment discharge and thus increased proportion of terrigenous sediments and freshwater proxies, and ii) change in dominating sedimentation regime with a typical predominance of widespread deposition from suspension due to development of large-scale

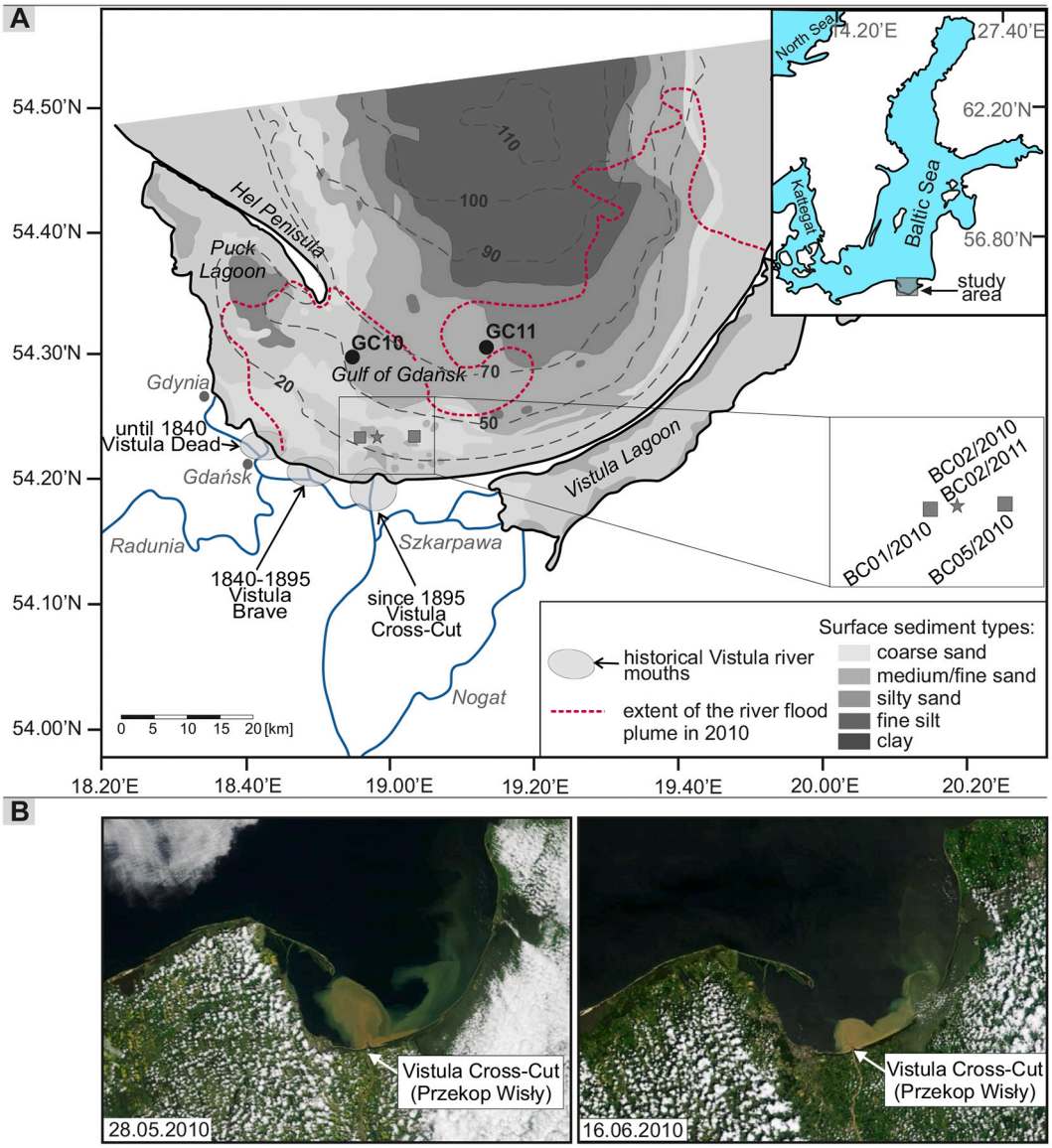

Fig. 1. Map of the study area. A) Map of the the Gulf of Gdańsk with the locations of coring sites. The distribution of dominating surface sediment types are after GeoLOG database (https://geolog.pgi.gov.pl/#name=53nv8rai9r). The map presents also the historical positions of Vistula River mouth, as well as the extent suspended sediment rich flood plume during the flood in 2010 (after Zajączkowski et al., 2010). The insets show the location of the Gulf of Gdańsk within Baltic Sea and names of the box cores collected next to the Vistula River mouth during the 2010 flood and one year later. B) Satellite images of the riverine flood plume entering the Gulf of Gdańsk in May and June 2010 from MODIS (Moderate Resolution Imaging Spectroradiometer) Aqua and Terra satellites (datasource: https://lance.modaps.eosdis.nasa.gov/). (For interpretation of the references to colour in this figure legend, the reader is referred to the web version of this article.)

freshwater/brackish, sediment-laden plumes (Fig. 1A-B). Among the freshwater proxies, diatoms were successfully used to study the sediment sources (e.g., Szczuciński et al., 2012). Therefore, we suggest that they may be a very useful tool in the studies of palaeoflood sediments. Diatoms are commonly occurring, photosynthetic organisms that inhabit diverse environments, including freshwater, brackish, and marine ecosystems. Species-specific sensitivity to the changes of many factors, including pH, temperature, nutrients concentrations, salinity, or water transparency, allows to use many diatom species as very accurate indicators of habitat conditions (Kolbe, 1927; Hustedt, 1939; Round, 1981; Denys, 1991; Vos and de Wolf, 1993). Previous studies showed that environmental fluctuations and catastrophic events like storms and tsunamis are well reflected in changes in diatom community structure (e.g., Kokociński et al., 2009; Szczuciński et al., 2012; Dura et al., 2016).

During the last 5000 years, the Gulf of Gdańsk was characterized by relatively stable conditions regarding changes in sea level and salinity. The previous studies on diatom flora preserved in sediments of the Gulf of Gdańsk focused mainly on temporal and spatial variability in paleoenvironmental conditions (Witkowski, 1994; Witak, 2000; Witak et al., 2006; Witak and Dunder, 2007; Leśniewska and Witak, 2008; Witak, 2010). However, changes in diatoms community structure have never been studied as a proxy to reconstruct flood events in this area. The aims of the present study were twofold: i) to determine the indicators of river floods deposits in marine sediments of the Gulf of Gdańsk, and ii) to examine the preservation of flood events in the sedimentary record in the context of palaeogeographical (variability in river mouth position) and palaeoclimatological changes (Vistula River flood frequency).

2. Regional setting

The Gulf of Gdańsk, located in the south-eastern part of the Baltic Sea (Fig. 1), has an area of ca. 4940 km^2, with an average depth of 59 m (Majewski, 1994) and a maximum depth of 110 m in the Gdańsk Deep (Uścinowicz et al., 1998). The Gulf of Gdańsk was predominantly shaped by the Pleistocene glaciations and the following erosional and accumulation processes, related mainly to sea-level changes (Uścinowicz, 2003, 2006; Uścinowicz et al., 2007; Witak, 2010, 2013a, 2013b) and sediment supply from the Vistula River. The latter is the longest river flowing into the Baltic Sea, with catchment including most of the territory of Poland (over 194,420 km^2). The modern sediments in the Gulf of Gdańsk mainly come from the Vistula River, coastal erosion, and human activity (Uścinowicz et al., 1998). Their grain size type is generally related to water depth (Fig. 1). The fine to coarse sands dominate in water depths less than 50 m, silty sand and silt are common down to approximately 70 m, and clay deposits in the deepest part (Jegliński et al., 2012).

The Gulf of Gdańsk is brackish with a salinity of up to 12 PSU in the deepest part and as low as 1 PSU near the Vistula River mouth (Kruk-Dowgiałło and Szaniewska, 2008). The alongshore currents dominate coastal water circulation. During the winter storms, the wavelengths reach 40–60 m (Damrat et al., 2013) and cause significant sediment redeposition from shallow waters. Damrat et al. (2013) estimated that more than two-thirds of the sediment mass deposited on the Vistula River prodelta may be redeposited to the deeper part of the Gulf of Gdańsk. The waters are eutrophic (Niemkiewicz and Wrzołek, 1998; Szymczak-Żyła and Kowalewska, 2009; Leśniewska and Witak, 2011; Voss et al., 2011; Szymczak-Żyła et al., 2019) and with low visibility, which limits the photic zone up to a few meters (Łysiak-Pastuszak et al., 2004; Witak and Pędziński, 2018). Moreover, during summer periods cyanobacteria blooms were frequently observed in recent decades (Pawelec et al., 2018; Pliński et al., 2007).

The present average Vistula River water discharge is 1080 m^3 s^{-1} (Pruszak et al., 2005) and ranges between 250 and 8000 m^3 s^{-1} (Cyberski et al., 2006). During normal conditions, the low-salinity riverine sediment-laden plume can reach a distance of 9–27 km (Grelowski and Wojewódzki, 1996), and its thickness may range from 0.5 to 12 m (Cyberska and Krzymiński, 1988). Heavy rains from the 15 to 17th of May, which resulted in some places in precipitation being over 350% higher than the monthly mean (Świątek, 2013), caused a major spring flood in 2010. During the flood, the river plume was up to 10 m thick and extended offshore as far as 70 km (Fig. 1), while the river water discharge was over 6800 m^3 s^{-1} (Zajączkowski et al., 2010).

The Vistula River forms a delta plain called the Żuławy Wiślane, and the primary river mouth/s position has changed with time. Throughout the Late Holocene, a significant part of the water and sediment discharge was delivered to Vistula Lagoon (Witak, 2013b), which nowadays is separated by the Vistula Spit from the Gulf of Gdańsk (Fig. 1). According to historical documents, the spit used to be divided by several cross-channels connecting the Vistula Lagoon with the Baltic Sea (Bertram, 1907; Bertram et al., 1924). The westernmost branch of the Vistula River, called Dead Vistula (Wisła Martwa) (Fig. 1), and located in the modern city of Gdańsk, was probably established already in the Neolithic times (Jegliński, 2013). In the period 1400 to 1840 CE, it was a major river mouth delivering annually around 100,000–150,000 m^3 of sediments (Jegliński, 2013). After a major river ice jam in 1840 CE, the primary river mouth shifted eastward and formed Vistula Brave (Wisła Śmiała) (Łomniewski, 1960). The last significant change was related to the formation of a new, artificial channel, the Vistula Cross-Cut (Przekop Wisły) in 1895 (Fig. 1), which has served as a major river mouth since then, and a new prodelta was built in front of the new river mouth (Koszka-Maroń, 2009).

The study area is characterized by a transitional oceanic-continental temperate climate affected by North Atlantic Oscillation (NAO) variations and westerly storm tracks (Börgel et al., 2018). During the Late Holocene, a period of predominantly warm and dry climate before ~2.3 kyr BP was followed by gradual cooling and wetting punctuated by several minor dry and warm spells (Lamentowicz et al., 2015; Pleskot et al., 2022). The peak cooling was reported during the Little Ice Age (LIA) at ~0.4 kyr but low temperatures persisted until the onset of post-industrial revolution warming.

The Vistula River floods are mainly generated by the following mechanisms: intense and/or long-lasting rain, snowmelt, ice-related phenomena, and storm surge (Cyberski et al., 2006). There are several records of historical Vistula River floods, mainly related to periods after the 14th century (e.g., Brandstäter, 1879; Bertram, 1907; Bertram et al., 1924; Cieślak and Bernat, 1969; Cyberski et al., 2006; Girguś, 2020). In general, the periods 1400–1560, 1620–1700, and 1800–1880 CE are reported to be characterized by higher flood frequency.

3. Materials and methods

The material for this study was collected during two cruises to the Gulf of Gdańsk (May 2010 and May 2011) with R/V Oceania of the Institute of Oceanology, Polish Academy of Sciences in Sopot, Poland. In 2010, hydrological and sedimentary conditions during a large Vistula river flood were documented (Zajączkowski et al., 2010). Surface samples were taken using a box corer at eight sampling stations in the water depth range of 20–30 m. Surface samples from 3 of them, with prominent fresh flood deposit layers, were investigated here (Table 1, Fig. 2). In 2011, the box core BC02 was taken from the same site as the previous year (Fig. 1). Moreover, two long piston cores were retrieved from the southern part of the Gulf of Gdańsk. Core GC10 was taken from a shallower part of the gulf, about 18 km off the present Vistula mouth, whereas core GC11 was from a deeper, central region, approximately 20 km from the modern river mouth (Fig. 1A). Detailed information on the sampling stations is provided in Table 1. The sediment cores were cut into two halves in the lab, X-rayed to reveal internal sedimentary structures, and described. The cores were sliced into 1-cm thick sediment samples for further analyses.

Table 1
Overview of the coring stations: core number, coring gear, sampling date, location, water depth, and core length.

Core number	Coring gear	Sampling date	Latitude	Longitude	Water depth [m]	Core length [cm]
BC01	Box corer	28.05.2010	54°23.243′ N	18°56.131′ E	20	15
BC02*	Box corer	28.05.2010 29.05.2011*	54°23.572′ N	18°58.838′ E	23	16
BC05	Box corer	28.05.2010	54°23.674′ N	19°3.927′ E	32	20
GC10	Piston corer	29.05.2011	54° 30.19′ N	18°55.1′ E	61	199
GC11	Piston corer	29.05.2011	54°31.649′ N	19°15.902′ E	76	227

* The site was resampled after one year.

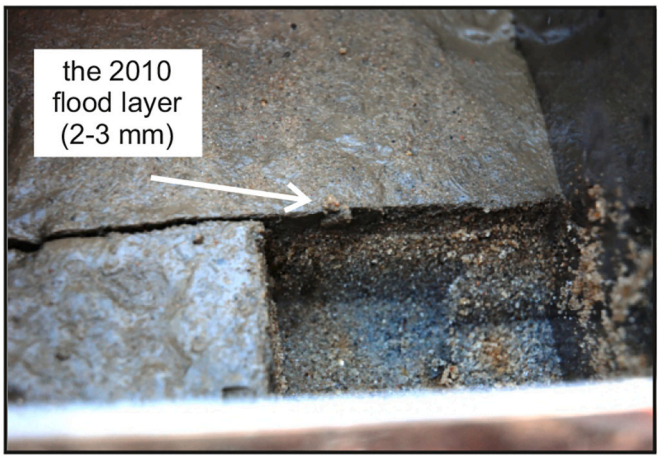

Fig. 2. Photograph of box core BC05/2010 collected from water depth of 32 m during maximum flood discharge of the Vistula River in May 2010. The freshly deposited surface layer is composed of poorly sorted silty medium sand.

3.1. Dating

The chronology of the studied cores GC10 and GC11 was based on accelerator mass spectrometry (AMS) ^{14}C dating performed on thirteen samples of the shells of marine bivalves (Table 2), supplemented with gamma spectroscopy measurements of ^{210}Pb and ^{137}Cs in the upper 20 cm of the cores (Supplementary Table 1). The AMS ^{14}C measurements were performed by Poznań Radiocarbon Laboratory, Poland (Goslar et al., 2004). The obtained ages were converted into calibrated years BP (cal. BP) with Calib 8.2 (Stuiver et al., 2022) using the Marine20 calibration curve (Heaton et al., 2020). The local correction for the reservoir age $\Delta R = -50 \pm 100$ years was applied (Szymczak-Żyła et al., 2019). Apparent sediment accumulation rates for approximately the last 100 years were determined using excess ^{210}Pb and verified with a penetration depth of anthropogenic ^{137}Cs isotopes (Robbins and Edgington, 1975). The excess ^{210}Pb was defined as a difference between the total ^{210}Pb and the average of ^{214}Pb and ^{214}Bi. These isotopes and ^{137}Cs were measured with germanium gamma detector GX2520 manufactured by Canberra and housed in the Institute of Geology, Adam Mickiewicz University, Poznań, Poland. The data were analyzed using the *serac* package (Bruel and Sabatier, 2020). They were also used to assess sediment loss from the core tops, which appeared to be minor (likely much less than 50 years of sedimentation). Age-depth models for the piston cores were constructed using the *rbacon* package version 2.5.6 (Blaauw et al., 2021) using R ver. 4.1.3, and were derived from all AMS ^{14}C dates. The *rbacon* package performs Bayesian age-depth modeling that includes the dating probability distribution. All the ages reported in the text are calibrated ages.

3.2. Sediment structure and texture (grain size analysis)

The studied sediments were described on board in the case of box cores and in the lab for long cores. The macroscopic description was supplemented by a description of structures visible in X-radiographs of 1 cm thick sediment slabs, made with a standard medical digital X-ray machine. The sediment grain size distribution was analyzed for 429 samples (3 surface samples, 227 samples from GC11, and 199 from GC10 core) by applying volumetric grain size analysis using laser beam diffraction. Before the investigation, samples were treated with dispersing fluid Calgon (a combination of sodium hexametaphosphate and sodium carbonate) and ultrasounds (30 s) to avoid grain aggregation. The analyses were performed on a Mastersizer 2000 Particle Size Analyzer by Malvern. The grain-size statistics were calculated with GRADISTAT (Blott and Pye, 2001) using the logarithmic method of moments.

Table 2
Results of AMS radiocarbon dating calibrated with Calib 8.2.

Core number	Sample depth [cm]	Lab No.	AMS ^{14}C [years BP]	Calibrated years BP [2-sigma range]
GC10	93.5	Poz-47004	920 ± 30	179–630
GC10	98.5	Poz-47005	970 ± 30	244–665
GC10	111.5	Poz-47006	1185 ± 30	450–882
GC10	115.5	Poz-47007	1200 ± 30	464–892
GC10	121.5	Poz-47008	1400 ± 30	617–1090
GC10	137.5	Poz-47010	1515 ± 30	708–1208
GC10	150.5	Poz-47011	1765 ± 30	950–1452
GC10	172.5	Poz-47012	2240 ± 30	1435–2008
GC10	184.5	Poz-47013	2250 ± 35	1454–2035
GC11	39.5	Poz-47000	1115 ± 30	355–797
GC11	48.5	Poz-47001	1200 ± 30	464–892
GC11	169.5	Poz-47002	4035 ± 35	3624–4268
GC11	176.5	Poz-47003	3805 ± 30	3362–3946

3.3. Geochemistry

The analyses of total carbon (TC), total organic and inorganic carbon (TOC and TIC), total nitrogen (TN), and total sulfur (TS) were conducted at the Department of Quaternary Geology and Palaeogeography of the Institute of Geoecology and Geoinformation at the Adam Mickiewicz University in Poznań, Poland. The analysis was performed for 40 homogenized samples using a Vario MAX CNS elemental analyzer (Elementar, Germany). To determine the TOC, before analysis samples were placed on silver foil and treated three times with one molar hydrochloric acid (HCl) to remove carbon bound in carbonates, considered to be TIC. Each sample was analyzed in duplicate. Analytical control was performed using certified reference materials (Woszczyk et al., 2021).

Assuming that TIC is bound in carbonates only, the TIC was multiplied by 8.33 to calculate the percent of calcium carbonate ($CaCO_3$).

3.4. Diatom analysis

Diatoms were analyzed in 122 samples collected from fresh 2010 flood event deposits and from the piston cores. The latter were sampled in regular intervals, every 5 cm, as well as in higher resolution, every 1 cm, in core sections suspected to represent flood events (characterized by bimodal grain size distribution with the additional secondary mode in silt fraction interpreted to be a result of direct deposition from hypopycnal river flood plume). Samples preparation followed standard methodology according to Battarbee (1986). At least 350–450 diatom frustules per sample were counted in immersion oil under an optical microscope (1000×) equipped with Nomarski contrast. Moreover, selected samples were analyzed under Scanning Electron Microscopy (SEM) at the Laboratory of Electron and Confocal Microscopy, Faculty of Biology, Adam Mickiewicz University, Poznań, Poland. The individual diatom species were identified following descriptions presented by Bąk et al. (2012), Witkowski (1994), Witkowski et al. (2000), Snoeijs and Potapova (1993, 1995), Snoeijs and Vilbaste (1994), Snoeijs and Kasperoviciene (1996), Snoeijs and Balashova (1998), and Krammer and Lange-Bertalot (1986, 1988, 1991a, 1991b). The diatom assemblages were grouped according to the salinity and environmental preferences after Kolbe (1927), Vos and de Wolf (1993), Van Dam et al. (1994), and Witkowski et al. (2000). Additionally, grouping according to the habitat followed https://www.algaebase.org/ database, www.diatoms.org and Round (1981). Moreover, https://www.algaebase.org was used to check all identified species names.

3.5. Statistical analyses

In order to determine the significant patterns and the correlation between grain size statistics (mean grain size, standard deviation, skewness, kurtosis) and diatom species grouped by their salinity (indifferent, halophilic, mesohalobic, euhalobic) and habitat (benthic, planktonic) preferences the principal component analysis (PCA) was conducted. Before the analysis, data were standardized to zero mean and unit variance. The analysis was run in R ver. 4.1.0 (R Core Team, 2021).

4. Results

4.1. Dating and age models

The gamma spectrometry measured activities of a total ^{210}Pb, supported ^{210}Pb, ^{137}Cs, and calculated excess ^{210}Pb ($^{210}Pb_{ex}$) are presented in Fig. 3 and Supplementary Table 1. In both cores, the top sections contained $^{210}Pb_{ex}$ and ^{137}Cs with downward decreasing activities, suggesting that the potential loss of the topmost sediment during the coring was limited. However, the lack of evidence of surface mixed layer in radionuclides depth profiles, as expected in the case of bioturbated sediments (e.g., Nittrouer et al., 1984), despite evidence of mixing visible in X-radiographs (Supplementary Fig. 2), might suggest that at least the upper several cm of sediment cores may be missing. Thus the calculated sediment accumulation rates must be treated as approximate only.

In the core GC10, the apparent sediment accumulation rate calculated with the ^{210}Pb-based CFCS model was 1.07+/− 0.07 mm yr^{-1} and was validated by ^{137}Cs penetration depth (Fig. 3A). In the core GC11, the $^{210}Pb_{ex}$ downward profile changed with depth (at c. 6 cm), suggesting a change in the sediment accumulation rate (Fig. 3B). The rates calculated with the CFCS model were 2.08+/− 0.09 mm yr^{-1} and 1.1+/− 0.07 mm yr^{-1}, for the upper and lower section, respectively. This model had some disagreement with the CIC model and the ^{137}Cs penetration depth; the latter isotope revealed very low activities down to at least 12 cm suggesting its remobilization or deep mixing. In the case of both cores, the ^{137}Cs maximum activity is at the surface and declines with depth, which may indicate that the profiles were not complete and/or the sediments were mixed.

The age model of the GC10 core was based on nine radiocarbon dates of marine shells, which were in stratigraphic order (Table 2, Fig. 3C). The core covered approximately 1600 years. The long-term averaged sediment accumulation rate for the older section of the core (> about 650 years BP) was 0.5 to 1.2 mm yr^{-1}; thus, 1 cm of the core accumulated in 8 to 20 years. In the younger section, the accumulation rate increased to 1–2 mm yr^{-1}, and in the period of approximately 280 to 610 years ago to an even higher rate of 1.5–3.3 mm yr^{-1}. Thus, in the younger part of the core, the 1 cm sediment section represented on average 3 to 10 years and generally agreed with the ^{210}Pb-based assessment.

The sediments retrieved in core GC11 were accumulated approximately over the last 4500 years. The age model was based on four samples (Fig. 3D). The average accumulation rate was 0.4 to 0.5 mm yr^{-1}, except for the last 700 years when it had increased to reach 0.7 mm yr^{-1} and approached the ^{210}Pb-based estimate of over 1 mm yr^{-1} during the previous century. The long-term accumulation rates resulted in moderate resolution, as a 1 cm thick sediment sample accumulated on average for 15–20 years.

4.2. Sediment properties

Among the investigated sedimentary properties of the deposits were grain-size characteristics (grain size distribution, mean grain size, sorting, skewness and kurtosis) analyzed in high resolution (every 1 cm) (Figs. 4 and 5; Supplementary Fig. 1; Supplementary Table 2), and sedimentary structures (Supplementary Fig. 2).

4.2.1. Shallow water surface samples

During the research cruise in the course of the river flood in May 2010, on the seafloor in a water depth of 20–32 m, a several millimeters thin, fresh, brownish silty sand layer was observed to overlain the light coarse sandy deposits (Fig. 2). The surface layer was considered to be flood deposits and consisted of poorly sorted silty sands (Fig. 4A). The contents of the fine sand fraction ranged from 80.7 to 91.3%, and of the silt fraction from 8.5 to 18.8%. Clay fraction was below 0.5%. The grain size distribution was positively skewed. This characteristic layer was not found during the follow-up cruise next year when surface and near-surface sediments were composed of coarse-grained sand.

4.2.2. Core GC10

The sediments of core GC10 were mainly composed of poorly to very poorly sorted sandy silts. The sand fraction ranged from 13.6 to 54.4% (average 31.9%) and the silt fraction from 43.1 to 76.8% (average 63.2%), while the clay fraction was between 2.5 and 9.5%. The major changes were related to relative sand and silt contribution. In the sediments deposited during approximately the last 600 years, the sand content oscillated between 20 and 35%. In the period of roughly 550 to 800 years BP, the sand content was the highest and was in the range of about 35 to 50%, while in the oldest sediments, its content generally varied between 25 and 40% (Fig. 5B). These changes were also reflected in grain size statistics. The coarser sediments were usually characterized by more positively skewed grain size distribution and better sorting.

Most of the samples revealed a unimodal and positively skewed grain size distribution (Fig. 4; Supplementary Fig. 1) with a mode in the fine sand fraction (129 samples, 65%) or the coarse silt fraction (70 samples, 35%). However, 5% of samples (n = 9) revealed a bimodal grain size distribution (Fig. 5), with the second mode in medium and fine silt fraction. The bimodal samples were characterized by the poorest sorting and were scattered throughout the core (Supplementary Table 2), except for the section deposited before approximately 1400 years BP.

The sedimentary structures (Supplementary Fig. 2) were dominated by remnants of layering altered by mixing and bioturbation throughout

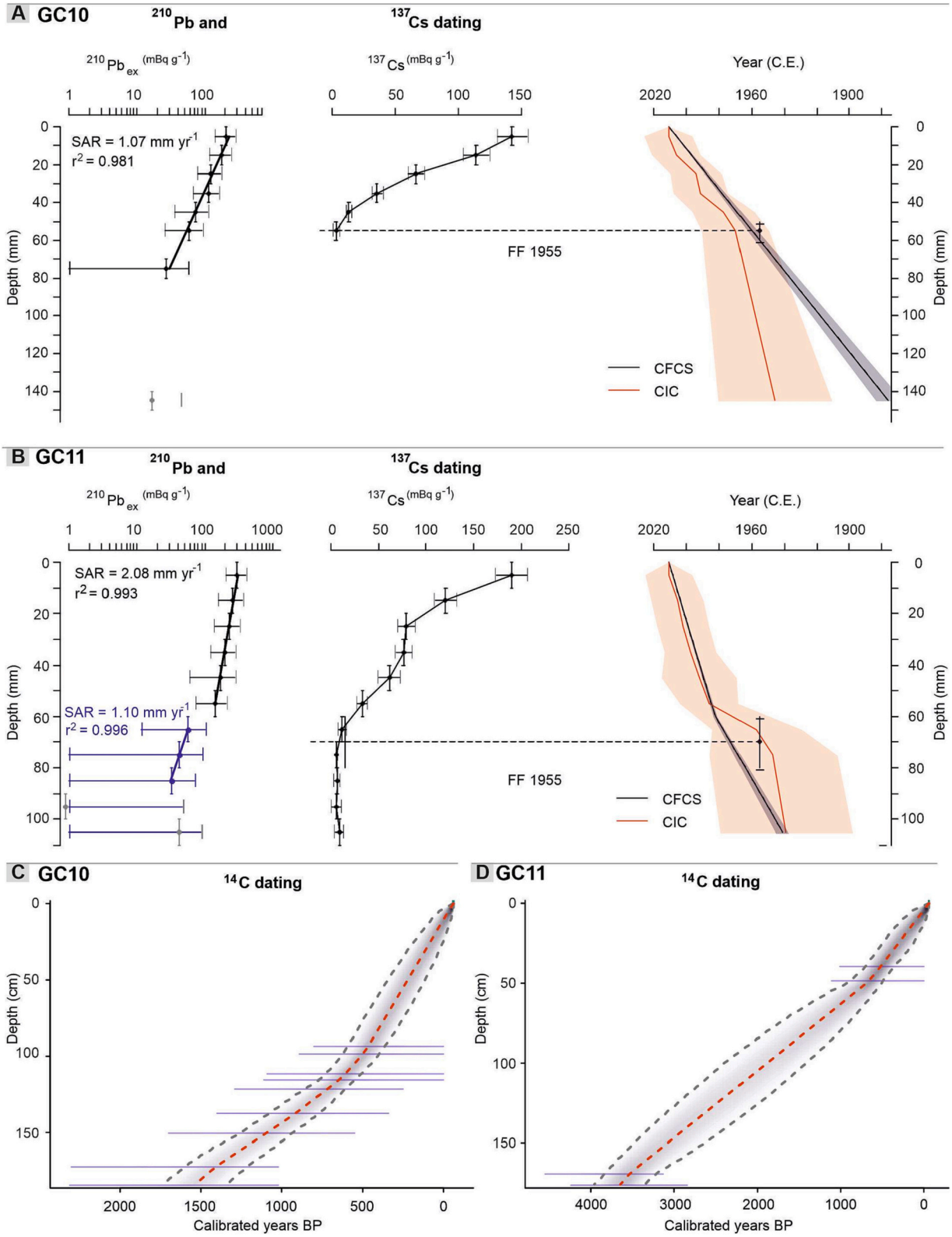

Fig. 3. Dating results and age models. A) and B) Short-lived radionuclides measurements and age-depth models for upper parts of the sediment cores GC10 (A) and GC11 (B). From left to right: $^{210}Pb_{ex}$ activity (semilogarithmic plot), ^{137}Cs activity, the CFCS (constant flux constant sedimentation rate) and CIC (constant initial concentration) age models. SAR – sediment accumulation rate, FF 1955 – First Fallout period, assessed by the decline of ^{137}Cs concentrations to near 0 mBq g^{-1}. The vertical error bars refer to analyzed sediment sample thickness, while the horizontal bars depict 2-sigma uncertainty. The figure was obtained in the *serac* R package (Bruel and Sabatier, 2020). C) and D) – Bacon-based (Blaauw et al., 2021) age-depth models derived from AMS ^{14}C dates. Calibrated ages are shown in transparent blue. The red curves show a single 'best' model based on the weight mean age for each depth. Black stippled lines show 95% confidence intervals. (For interpretation of the references to colour in this figure legend, the reader is referred to the web version of this article.)

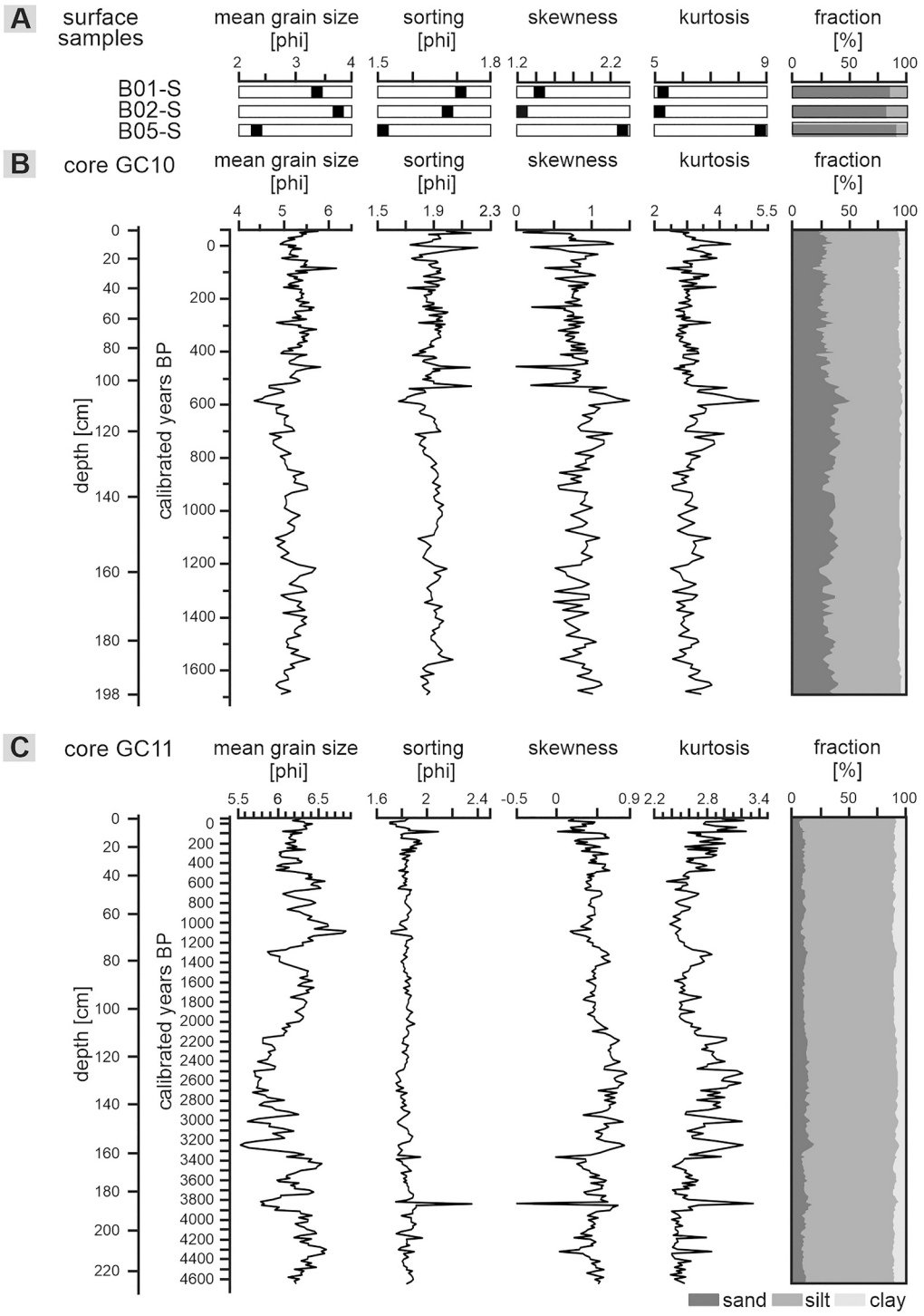

Fig. 4. Grain-size statistics and content of sand, silt, and clay fraction recorded in A) the surface, shallow-water, 2010 flood deposits, B) core GC10, and C) core GC11.

the core. Occasionally, fine-scale lamination was preserved.

4.2.3. Core GC11

The sediments of core GC11 were poorly sorted silts and sandy silts. The sand fraction ranged from 4.2 to 22.1% (average 10.8%) and the silt fraction from 72.4 to 85.2% (average 80.2%), while the clay fraction ranged from 5.3 to 11.8%.

The downward changes in the sediment grain size were well expressed by relative sand content, presented below, correlated to mean grain size and skewness (Fig. 4C). During the last approximately 970 years, the sand content varied between 6.5 and 13.5%, with the highest content between 220 and 520 years BP. Between around 910 and 1150 years BP, the sand content was the lowest (4.4 to 10%), while during the preceding period (c. 1150 to 1385 years BP) was much higher (11–15%). In the periods of approximately 1385 to 2100 years BP and between 3300 and 4700 years BP, the sand content was similar to the modern and was in ranges of 6.8–12.2% and 7.5 to 17.5%, respectively. The highest sand content was documented for approximately 1200 years long period from 2100 to 3300 years BP when sand fraction contained in the sediments reached 10.5 to over 22%.

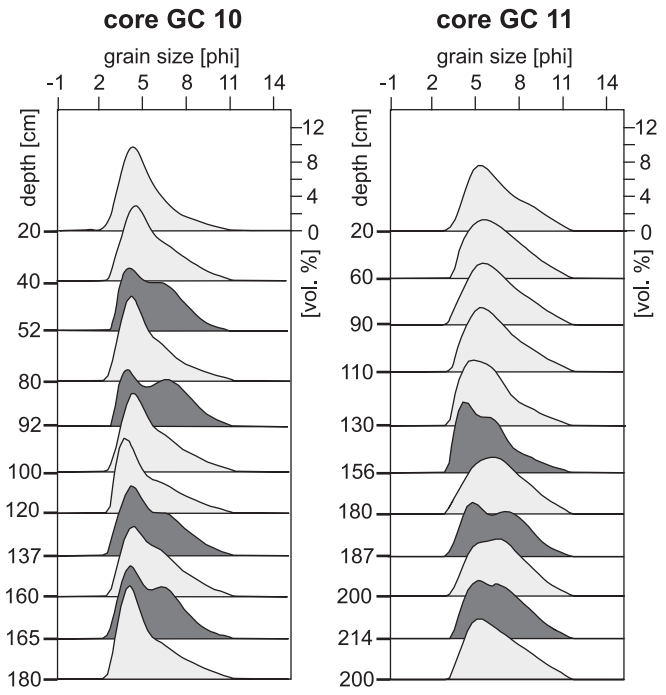

Fig. 5. Examples of grain size distributions of samples from cores GC10 and GC11. The bimodal distributions are marked with darker silhouettes. The grain size distributions for all 429 samples are presented in Supplementary Fig. 1.

Most samples (96%) were characterized by unimodal symmetrical or positively skewed grain size distributions. The bimodal grain size distribution was documented in seven samples (Supplementary Table 2), scattered in the core section older than 2800 years BP.

Throughout the core, the sedimentary structures visible in X-radiographs (Supplementary Fig. 2) were dominated by remnants of layering altered by mixing and bioturbation. The layering was better preserved in sediments older than circa 2300 years BP.

4.3. Sediment geochemistry

Sediment geochemistry data, namely percentages of TC, TOC, TN, TS, and $CaCO_3$ (calculated from TIC), were presented in Fig. 6 and Supplementary Table 3. The fresh thin layer of flood sediment from 2010 showed values in ranges of 0.73 to 1.55% (TOC), 0.08 to 0.16% (TN), 0.03 to 0.14% (TS), and 0.41–0.79% (calcium carbonate).

In the cores GC10 ($n = 19$) and GC11 ($n = 18$), the variations of the analyzed compounds were moderate, except for the core top samples, which were characterized by much higher contents of TOC, TN, and CaCO3, and lower TS content (Fig. 6). In the GC10 core, the TOC content ranged from 0.96 to 3.13%, and reached 4.03% in the surface sample. The TN and TS were respectively in ranges of 0.18–0.3% and 0.67–1.6%, while the surface sample contained 0.96% of TN and 0.66% of TS. The $CaCO_3$ content in the surface sample was 7.3%, while it ranged from 0.37 to 2.65% downcore. In the core GC11, the TOC ranged from 3.37 to 4.78% and reached 5.98% in the surface sample. The TN was between 0.33 and 0.53% and as high as 1.31% in the surface sample. The contribution of TS was in the range of 1.23 and 2.07%, except for the surface sample (0.64%). The $CaCO_3$ in the GC11 core ranged from 1.36 to 5.66% and was doubled in the surface sample (11.30%).

The TOC/TS ratio, used as an approximate indicator of sediment redox (Berner, 1984), was between 6 and 26 in the surface sediments collected in 2010 and the top core samples and indicated fully oxic conditions. Downcore, the values ranged from 1.4 to 3.8, characteristic for periodically anoxic conditions.

4.4. Diatom analysis

The diatom analysis was conducted for samples collected from shallow-water surface 2010 flood deposits ($n = 3$) and the cores GC10 ($n = 62$) and GC11 ($n = 57$). In samples of 2010 surface flood deposits, 55 taxa were recognized, and 41 of them were benthic. One hundred forty-five taxa were identified in the piston cores, 125 benthic and 20 planktonic. Considering environmental preferences, 32 euhalobous, 31 mesohalobous, 15 oligohalobous halophilus, and 67 oligohalobous indifferent taxa were recognized. The results are presented in Figs. 7-9 and detailed diatom counts are in Supplementary Table 4.

4.4.1. The 2010 flood surface deposits

The diatoms found in shallow-water surface sediment samples (BC01, BC02, and BC05) collected during the flood in 2010 contained mainly planktonic diatoms (over 80%). The most common species, belonged to genera Cyclotella (*C. atomus*), Stephanocyclus (*S. meneghinianus*), Stephanodiscus (*S. parvus, S. hantzschii*), and Thalassiosira (*T. angulata, T. baltica, T. oestrupii*). Among the benthic diatom species most common were Diatoma (*D. tenuis, D. vulgaris*), *Tryblionella apiculata, Staurosirella pinnata* and *Staurosira construens*. Oligohalobous

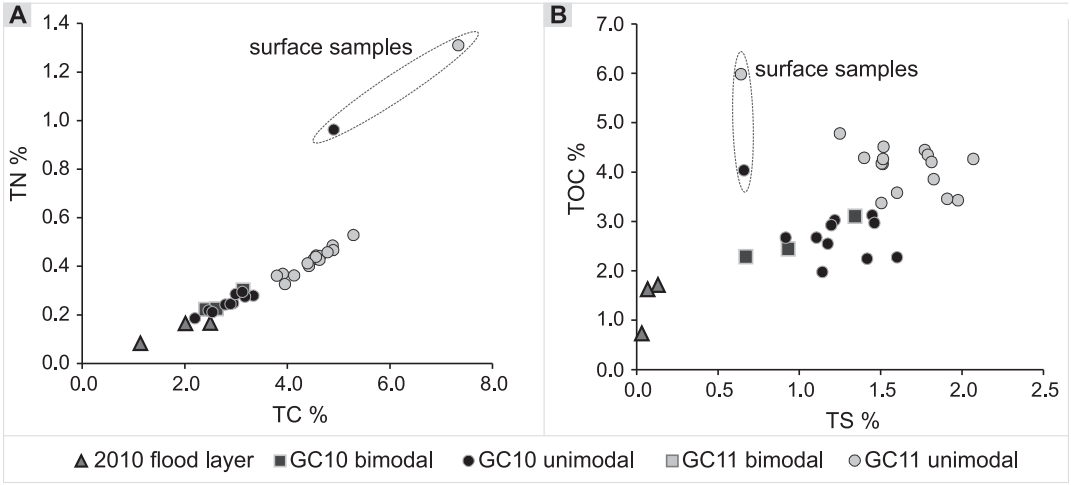

Fig. 6. The sediment geochemistry expressed as total nitrogen (TN), total carbon (TC), total organic carbon (TOC), and total sulfur (TS). The analyzed samples were assigned to fresh flood layers collected in 2010 ("2010 flood layer") and to samples that were characterized by unimodal and bimodal grain size distributions from cores GC10 and GC11 (see Fig. 5). The two outlined outliers were the cores surface samples.

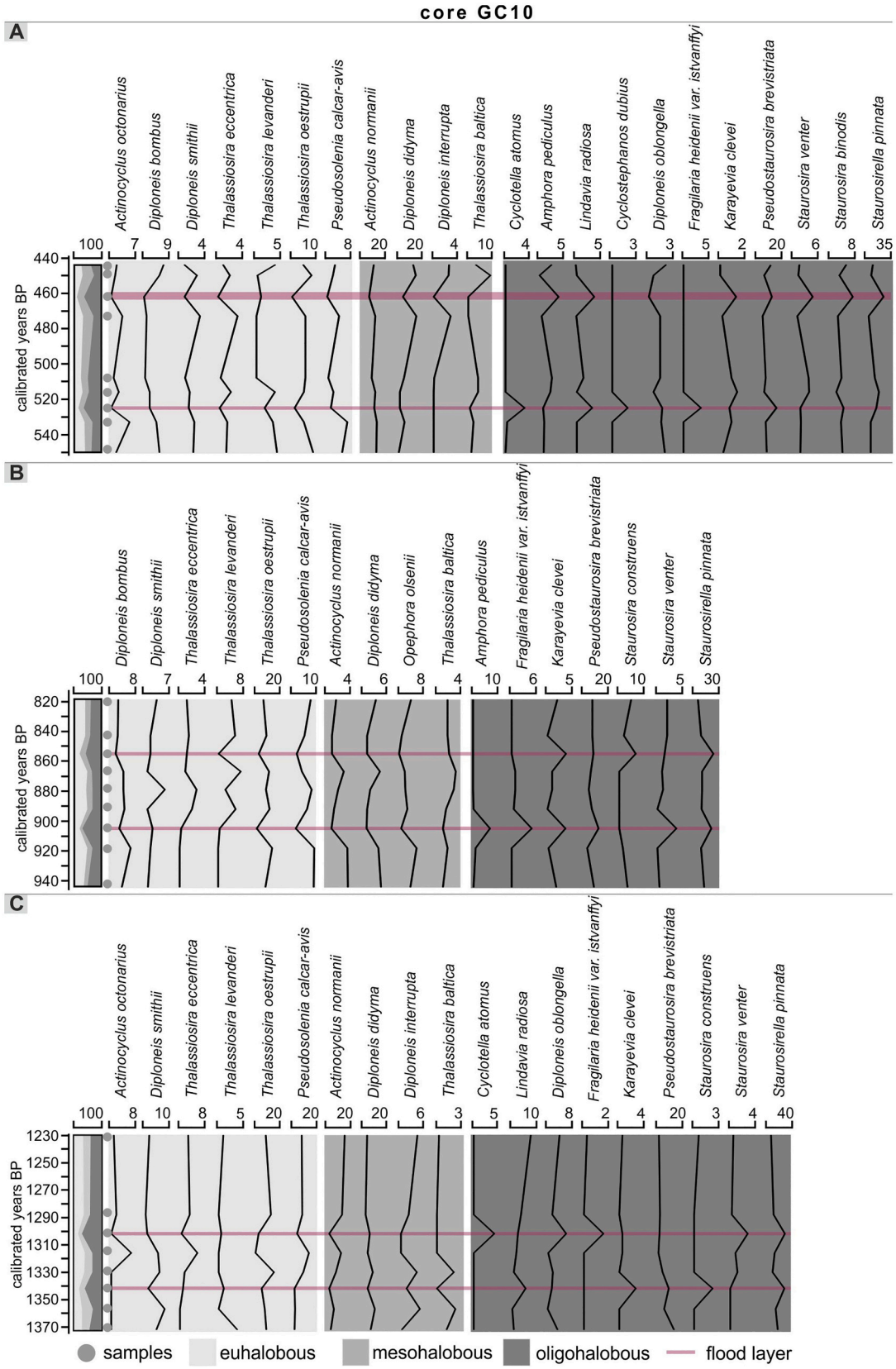

Fig. 7. Contribution (%) of diatom salinity groups and dominant diatom taxa in core GC10 for the depth ranges: A) 90–105 cm (440–550 years BP), B) 130–140 cm (820–940 years BP), C) 160–170 cm (1230–1370 years BP). The layers characterized by bimodal grain size distribution and interpreted to be "flood layers" are marked with pink lines. (For interpretation of the references to colour in this figure legend, the reader is referred to the web version of this article.)

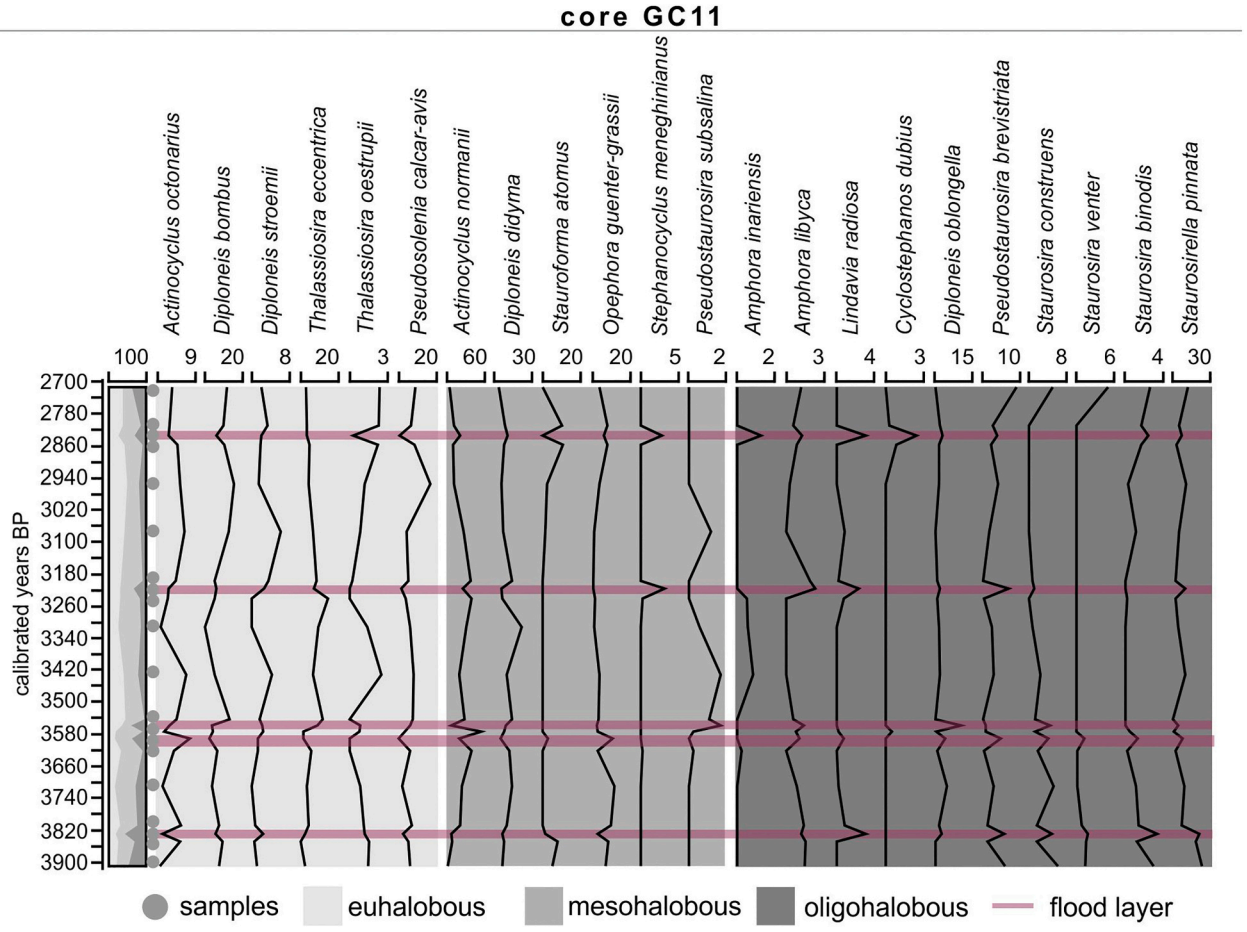

Fig. 8. Contribution (%) of diatom salinity groups and dominant diatom species in core GC11 for the depth range 135–190 cm (2700–3900 years BP). The layers characterized by bimodal grain size distribution and interpreted to be "flood layers" are marked with pink lines. (For interpretation of the references to colour in this figure legend, the reader is referred to the web version of this article.)

halophilus and indifferent species constituted 81 to 93% of all the species, while, on average, halophilus species contributed 53%, and indifferent taxa 33%.

4.4.2. Core GC10

In core GC10, 115 taxa were identified (Supplementary Table 4), including 28 euhalobous, 27 mesohalobous, 12 oligohalobous halophilus, and 48 oligohalobous indifferent taxa. Benthic diatoms content varied between 29.7 and 96.6% (71.3% on average), while planktonic between 3.4 and 70.3% (28.7% on average). Euhalobous diatoms constituted from 7.7 to 59.9% (31.3% on average), mesohalobous 3.8 to 43.6% (22.6% on average), oligohalobous halophilus up to 15.8% (4.1% on average) and oligohalobous indifferent 23.1 - 67.8% (42% on average).

General diatom species composition changes revealed three major stages underlined by the modest variability in the relative contribution of diatom groups with particular environmental preferences. The youngest stage, from about 500 years BP to the present, was characterized by slightly lower content of euhalobous diatoms and enrichment in oligohalobous taxa. The second period, from approximately 1200 to 500 years BP, was marked by a higher content of euhalobous diatoms. The oldest sediments (approximately 1700 to 1200 years BP) were enriched in mesohalobous diatoms (Fig. 9).

Euhalobous diatoms in this core were dominated by *Pseudosolenia calcar-avis*, *Thalassiosira levanderi,* and *Actinocyclus octonarius*. Their relative contributions ranged from 0 to 14.6%, 0 to 47%, and 0 to 11%, respectively. Major downcore variations were noted for *P. calcar-avis*, which was rare during the last about 250 years, and much more common in the older deposits. In contrast, the contributions of *T. levanderi* and *A. octonarius* were much higher during the last 250 years, while their content was much lower and relatively stable in the older core section (Supplementary Table 4). Mesohalobous diatoms were dominated by *Actinocyclus normanii* and *Opephora olsenii* while oligohalobous by *Pseudostaurosira brevistriata* and *Staurosirella pinnata*.

In contrast to less pronounced major long-term trends, very distinct changes in the contribution of various diatom groups were observed in high-resolution analyses of samples characterized by bimodal grain size distribution (considered as flood deposits) and adjacent samples with unimodal grain size distribution. The analyzed sediment layers with bimodal grain size distribution were at the following depths: 52 cm (~230 years BP), 92–94 cm (~450–460 years BP), 102 cm (~525 years BP), 133 cm (~855 years BP), 137 cm (~905 years BP), 165 cm (~1300 years BP) and 168 cm (~1340 years BP) (Fig. 7). The content of benthic diatoms in these core intervals was relatively higher, ranging from 79 to 94%. The contributions of euhalobous and mesohalobous diatoms in bimodal grain size distribution samples were lower by up to 20%, than in the surrounding sediments. These samples with bimodal grain size distribution revealed noticeable decrease in the following diatoms: *Actinocyclus octonarius*, *Diploneis (D. bombus, D. smithii), Tryblionella apiculata, Thalassiosira (T. eccentrica, T. levanderi, T. oestrupii, T. angulata), Grammatophora oceanica* and *Pseudosolenia calcar-avis* among euhalobous, and *Actinocyclus normanii*, *Pseudostaurosiropsis geocollegarum, Thalassiosira baltica*, *Diploneis didyma* and *Diploneis interrupta* among mesohalobous (Fig. 7). On the contrary, the opposite trend was

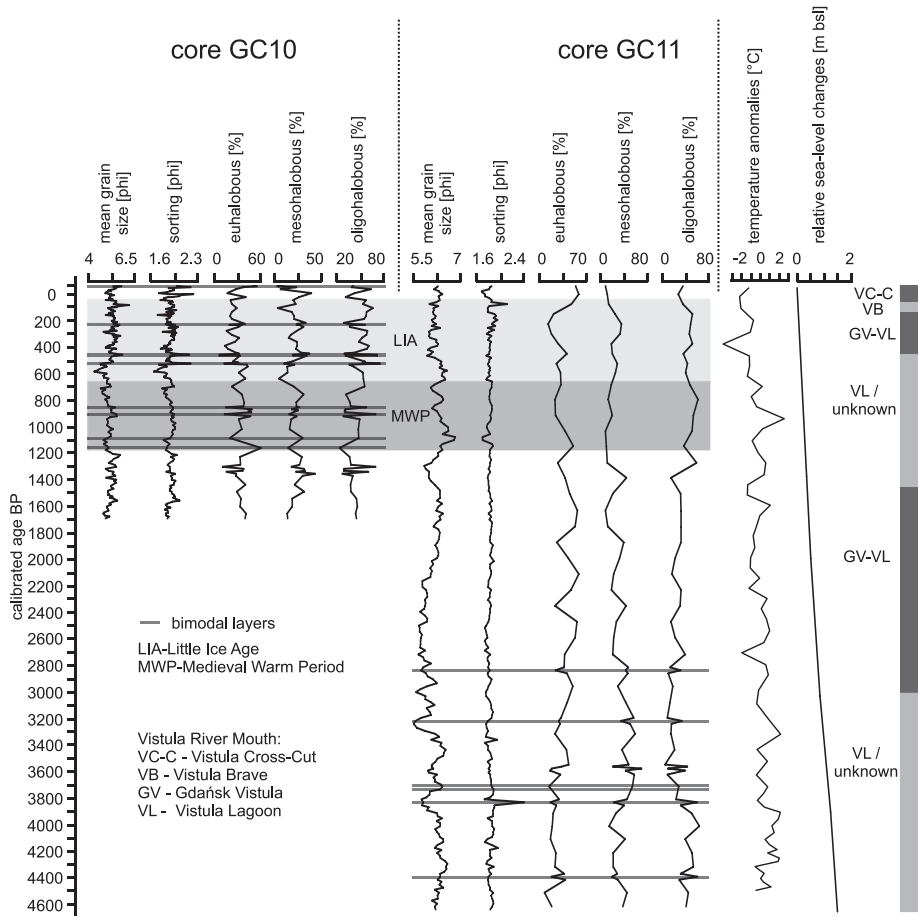

Fig. 9. Summary of the main results from cores GC10 and GC11 (mean grain size, sorting, contribution of major diatom groups) compared with temperature (Pleskot et al., 2022) and sea level (Uścinowicz, 2006) reconstructions, as well as with existing data on main Vistula River mouth position (Łomniewski, 1960; Cyberski, 1995; Witak, 2010; Jegliński, 2013; see Fig. 1 for their locations).

observed in the content of oligohalobous halophilus as well as indifferent species. Their contents were, in general, higher in samples with bimodal grain-size distribution, than in the surrounding sediments, and reached up to 70% of the total relative abundance. In particular, in case of Staurosirella and Pseudostaurosira genera. For instance, the contents of *Staurosirella pinnata* and *Pseudostaurosira brevistriata* were increased by 19–30% and by 1–10%, respectively. The contribution of the other freshwater diatoms, e.g. *Staurosira construens*, *Staurosira binodis*, *Staurosira venter* was increased by 1–5%. The contributions of diatoms belonging to *Actinocyclus* (*A. normanii* f. *subsalsus*), *Cyclotella atomus, Stephanocyclus meneghinianus*, *Navicula meniscus*, *Lindavia radiosa*, *Cyclostephanos dubius*, *Epithemia frickei*, *Staurosira inflata* and *Fragilaria heidenii* var. *istvanffyi*, in unimodal grain size distribution samples were below 1%, while in the bimodal grain size distribution samples their contents were up to 5%.

4.4.3. Core GC11

In core GC11 were recognized 123 diatom taxa, including 29 euhalobous, 22 mesohalobous, 13 oligohalobous halophilus, and 59 oligohalobous indifferent taxa. The content of benthic diatoms varied between 31.5 and 89.9% (63.1% on average), while planktonic was between 10.1 and 68.5% (36.9% on average). Euhalobous diatom constituted from 9.1 to 58.9% (33.8% on average), mesohalobous 9.2–69.5% (31.4% on average), oligohalobous halophilus up to 11.3% (2.4% on average) and oligohalobous indifferent 5.6–63.7% (32.4% on average).

The general trends in the contribution of diatom assemblages revealed four major periods. During the youngest c. 200 years, an increasing contribution of euhalobous diatoms was observed, reaching its maximum content in the core tope sediments. During the same period, the contributions of mesohalobous and oligohalobous groups revealed a decrease in the youngest sediments. The second period was dated to approximately 150 to 1300 years BP. The euhalobous and mesohalobous diatoms revealed relatively low stable contributions, while the content of oligohalobous diatoms was relatively high. The third period, dated back to approximately 2800 years BP, was characterized by small variability. However, the contributions of euhalobous and mesohalobous diatoms were slightly higher than in the second period, and the content of oligohalobous diatoms was lower. The oldest period (approximately 2800–4600 years BP) was characterized by the relatively stable moderate contribution of mesohalobous diatoms, while the content of euhalobous and oligohalobous diatoms respectively decreased and increased with the sediment age (Fig. 9). Dominant species in core GC11 were similar to core GC10. Dominant euhalobous diatoms in this core were *P. calcar-avis*, *T. levanderi* and *A. octonarius*. Mesohalobous diatoms were dominated again by *A. normanii, D. didyma, Opephora guenter-grassii* and *O. olsenii* while oligohalobous by *P. brevistriata, S. binodis* and *S. pinnata*.

Similarly to core GC10, higher variability in the contribution of various diatom groups was observed in high-resolution analyses of samples characterized by bimodal grain size distribution, considered as flood deposits, and adjacent samples with unimodal grain size distribution, than in case of general long-term trends (Figs. 8 and 9). The analyzed sediment layers with bimodal grain size distribution were at the depths: 140 cm (~2835 years BP), 156 cm (~3220 years BP), 171 cm (~3560 years BP), 173–174 cm (~3590–3610 years BP), 186 cm

(~3830 years BP) and 214 cm (~4390 years BP). The content of benthic diatoms in these layers ranged from 55 to 81% and was higher than in the surrounding sediments.

The samples with bimodal grain size distribution were characterized by lower than in the surrounding sedimets content of euhalobous and mesohalobous diatoms (in range of 3–22%). The most abundant euhalobous diatoms were represented by *P. calcar-avis, T. eccentrica, D. bombus*, *D. smithii* and *A. octonarius* while mesohalobous by *A. normanii*, *D. didyma, S. atomus* and *O. guenter-grassii*. However, contributions of these taxons varied significantly. For instance, content of *A. normanii* in the unimodal samples was up to 58%, and decreased in each bimodal sample by up to 8.4%.

The contents of diatoms representing oligohalobous halophilus and indifferent groups were, in general, higher in samples with bimodal grain size distribution than in the surrounding sediments, and reached up to 36.9% of the total relative abundance. Oligohalobous halophilus diatoms were represented by *Stephanocyclus meneghinianus*, which was detected only in the bimodal samples, *P. subsalina, S. pinnata, P. brevistriata, S. binodis, S. venter* and *S. construens*. Among of them *S. pinnata* revealed contents up to 25% content in each bimodal sediment sample.

4.5. PCA results

Principal component analysis (PCA) biplots showed the relationship between grain size distribution statistics and diatom groups in the sediment cores samples (Fig. 10). The first two axes of PCA explained 64.2% (grain size statistic and diatom groups included) and 79.2% (grain size statistic not included) of the total variance of observations in GC10 core. In GC11 core these values were 58.7 and 85.7%, respectively.

In both cores indifferent (freshwater) diatoms were related to the mean of grain size (Mz) and were represented mostly by benthic forms while the euhalobic (marine) diatoms were represented by planktonic forms. In GC10, the PCA analysis gathered the bimodal samples in one

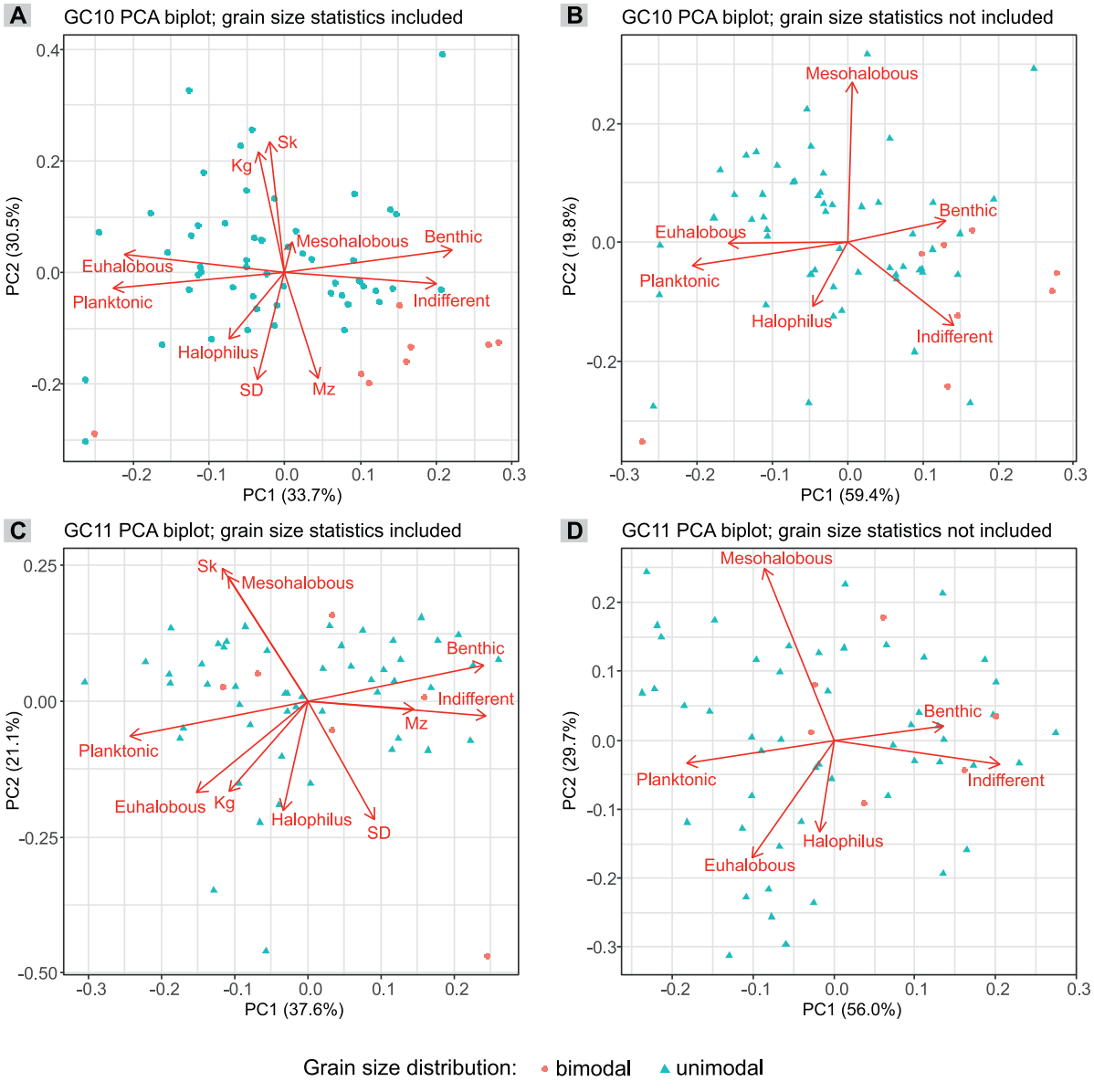

Fig. 10. Principal component analysis (PCA) biplots derived from GC10 (A) and B)) and GC11 (C) and D)) sediment core data. A) and C) show biplots derived from PCA run on combined diatom and grain size data, whereas B) and D) present biplots derived from PCA run solely on diatom data. The site scores are colored according to the grain size distribution of the sediment with bimodal samples marked in red and unimodal in blue. Variance explained by PC axes is provided in brackets. (For interpretation of the references to colour in this figure legend, the reader is referred to the web version of this article.)

group distributed along with contribution of indifferent diatoms.

PCA analysis based on data without grain size statistics distinguished in both cores indifferent diatoms as a separate group correlated with benthic diatoms. In core GC10, the bimodal samples were clustered as a separate group with the highest contribution of indifferent diatoms, while it was not clearly observed in core GC11.

5. Discussion

5.1. Identification of flood deposits

River flood deposits in marine sediments are known from various depositional settings, e.g., Eel shelf off California (Wheatcroft et al., 1997; Bentley and Nittrouer, 2003; Hill et al., 2007), Gulf of Mexico (Carlin et al., 2021), Gulf of Eilat-Aqaba, Red Sea (Mathalon et al., 2019), Adriatic Sea (Wheatcroft et al., 2006; Miserocchi et al., 2007), Mediterranean Sea (Mulder et al., 2001; Ducassou et al., 2008), or central Vietnam shelf (Szczuciński et al., 2009). However, their presence, preservation, and type vary greatly and depend on the amount of the flood-supplied material, the shape and oceanography of receiving basin, and postdepositional processes (e.g., Bentley and Nittrouer, 2003). The marine flood deposits may result from hyperpycnal flows and turbidity currents as known, for instance, from the Mediterranean Sea (e.g., Mulder et al., 2001). Flood layers are also known to form an event layer in the mid-shelf mud belt, as known from the Eel margin (Sommerfield and Nittrouer, 1999) or Vietnam shelf (Szczuciński et al., 2009), however, in these cases, the deposits were not directly delivered from the rivers, but they were likely redeposited from shallow water by wave-supported sediment gravity flows (Traykovski et al., 2000). In some sediment-starved depositional settings, the floods are interpreted from the increased sediment accumulation rates and environmental indicators instead of evidence of particular layers (e.g., Mendes et al., 2020). On the other hand, in high-energy depositional settings, where sediments are subjected to multiply redeposition due to waves, tides, and currents, the preservation of particular flood event layers is unlikely. Taking into account the variability of settings and environmental factors, it is clear that there is no single universal indicator of river flood deposits in marine sediments. Although, it is common to find the deposits to be fine-grained, enriched in terrigenous fingerprints (e.g., terrigenous organic matter), with preserved laminations or characteristic profiles of short-lived radionuclides (e.g., Sommerfield and Nittrouer, 1999).

5.1.1. River affected depositional system of Gulf of Gdańsk

The depositional environment of the Vistula River prodelta is the one with a low to moderate sediment supply. The latter could be more significant in the past, as a rapid decrease in the sediment transport was caused by the construction of dams (e.g., Włocławek) and changes in land use in the river basin (Lajczak, 2003). In normal conditions, the sediments delivered by the river are usually deposited close to the river mouth, as bedload (Lisimenka and Kubicki, 2019), as well as settling from a surface sediment-rich plume, which generally extends a few km offshore (Damrat et al., 2013). A large part of these deposits is redeposited into deeper water by the combined action of waves and currents (Damrat et al., 2013). However, as observed during the flood in 2010 (Zajączkowski et al., 2010), during the large flood events, the surface sediment-rich plume may extend for several tens of km offshore (Fig. 1) and lead to the deposition of a portion of riverine sediments with associated contaminants far offshore (e.g., Saniewska et al., 2014).

Consequently, in the context of supply and deposition of Vistula river sediments in the deeper part of the Gulf of Gdańsk, two depositional modes may be observed (Fig. 11). The more common, "normal" mode is the deposition of the riverine and coastal sediments in the shallow water (<30 m water depth), above the storm wave base. This kind of deposition takes place during normal conditions, but also during floods (Fig. 2). Part of the coarser deposits is accumulated and build up the proximal prodelta (Wróblewski et al., 2015), while the finer fraction of these deposits is in the majority redeposited by wave and current-induced near-bottom flows to the deeper part of the Gulf of Gdańsk (Damrat et al., 2013).

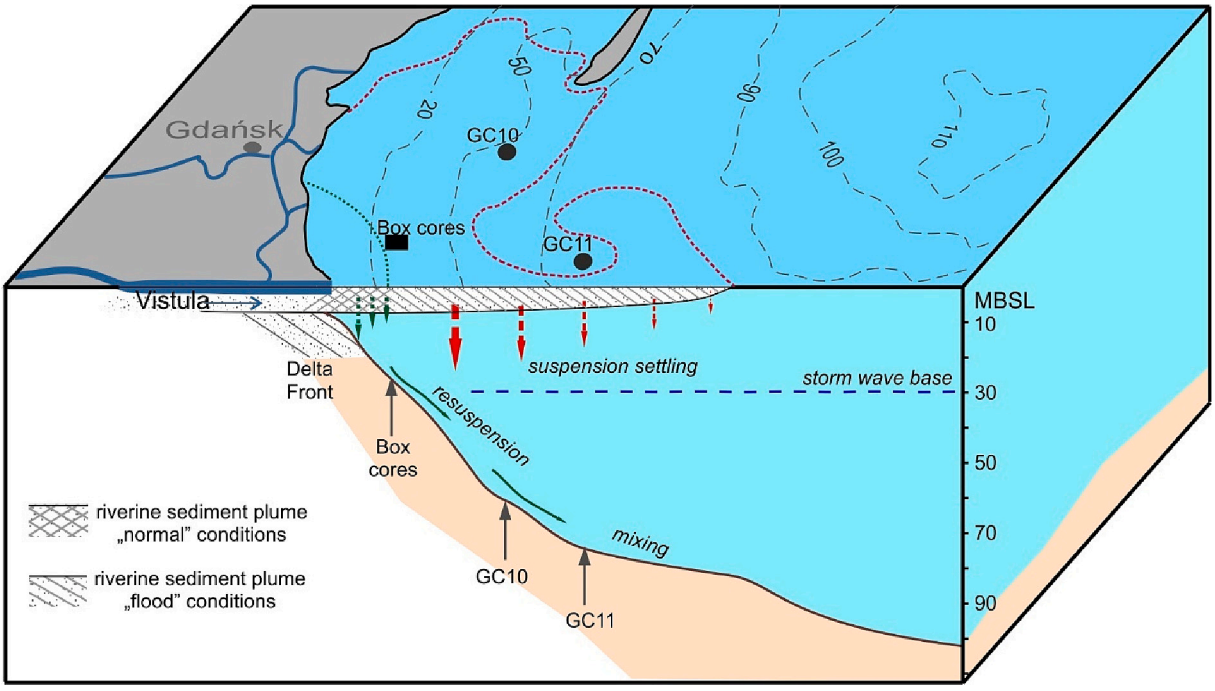

Fig. 11. A schematic block diagram illustrating a simplified model of the Vistula river depositional system in "normal" and large flood conditions. The bedload sediment transported by the Vistula river builds the delta. In contrast, the finer sediments deposited in the water depths above the storm wave base are resuspended, mixed, and in a significant amount transferred to the deeper parts of the Gulf of Gdańsk. The riverine sediment plume during the large floods extended further offshore, and suspended sediments settled down directly to the seafloor.

The second depositional mode is related to large flood conditions when surface water hypopycnal plume (brackish and suspended sediment-rich) extends much further offshore, up to 70 km during the flood in 2010 (Fig. 1, Zajączkowski et al., 2010), and leads to direct deposition of sediment not only close to the river mouth (in shallow water depths) but also more offshore in the deeper water depths. The deposits settled down from the plume represent much finer sediment grain size and properties of the riverine sediment source. The sedimentation rate from the hypocycnal plume decreases exponentially with the distance from the river mouth (Bursik, 1995). The sediment settled down in the shallow water is likely to be mixed and redeposited in the same way as the dominating mode of sediment dispersal.

5.1.2. Sedimentological evidence of flood deposits

During the 2010 flood, a thin silty sand layer (~3 mm) of flood deposits was observed (Fig. 2). The layer was deposited rapidly, as revealed by sediment trap measurements conducted in situ during the flood - the particulate matter flux was in the order of 35 g m^{-2} d^{-1} (Zajączkowski et al., 2010). These deposits were absent in the following year. The rapid deposition of riverine sediments nearby the river mouths, facilitated by flocculation, during high discharge events, and the subsequent redeposition of these sediments in following months due to high waves, storms, etc., is commonly observed worldwide. For instance, on the Eel continental shelf, the sedimentation from surface riverine flood sediment-rich buoyant outflow takes place mainly in the water depth of <20 m, while the flood deposits depocenter is at mid-shelf (50–100 m) (Hill et al., 2007). Similar post-depositional remobilization of fresh flood deposits was reported from the Gulf of Eilat-Aqaba (Mathalon et al., 2019), the Vietnam shelf (Szczuciński et al., 2009), and the Gulf of Mexico (Carlin et al., 2021).

The record of the flood deposits in the deeper water (60–80 m) sediment cores was not evident from sedimentary structures, as it was observed on the Eel continental shelf (Sommerfield and Nittrouer, 1999) or in the Adriatic Sea (Wheatcroft et al., 2006). It was likely partly due to the sediment mixing documented in X-radiographs and the relatively small amount of sediments settled down directly from the riverine plume. However, deposition of several mm thick flood lamina on the seafloor, even in case of its further mixing, may affect the grain size distribution. Indeed, within the studied cores analyzed in 1 cm resolution, we may observe most of the samples to be unimodal. However, some were bimodal, with an additional mode in the medium and fine silt fractions (Fig. 5). The later samples are preliminarily interpreted to result from combined ambient sedimentation due to the redeposition of sediments from shallower waters and direct settling from hypopycnal riverine plume (Fig. 11).

The 2010 flood is not recorded in the studied sediment cores. It is most likely due to core top loss due to piston coring in 2011. However, it may also be due to the smaller amount of sediment delivered by the flood than in the case of older large floods, which took place before river damming. Assuming that bimodal samples with poor sediment sorting reflect the significant flood events, we identified records of sixteen "flood layers", 9 and 7 in GC10 and GC11, respectively. The fine-grained fraction mode in these samples was always the secondary one, suggesting that the contribution of the deposits from direct settling from the riverine hypocynal plume was equivalent to less than 50% of 1 cm thick samples. Thus, possibly the original flood lamina, before sediment mixing, was thinner than 5 mm. Nevertheless, in PCA analysis, these flood layers differed from the remaining samples (Fig. 10). Regarding geochemical composition (TOC, TS), the bimodal deposits were not significantly different from ambient deposits (Fig. 6).

5.1.3. Diatom evidence of flood deposits

Several factors may cause the bimodal grain size distribution, including various sediment sources and sedimentary processes (e.g., Sun et al., 2002; Szczuciński et al., 2012). Thus, although the above explanation of the bimodal samples to be flood-affected layers seems plausible, it needs to be verified with another proxy. Among various applied indicators were micropaleontological proxies, for instance, foraminifera (e.g., Mendes et al., 2020) and applied here diatoms. The latter has been widely used to track environmental changes or detect extreme events, including tsunamis, hurricanes, or storms (e.g., Dura et al., 2016).

In the fresh layer of 2010 flood deposits temporarily left in shallow water, most of the diatoms were planktonic. The diatom assemblage was mainly composed of freshwater species from Cyclotella (*C. atomus)*, Stephanocyclus (*S. meneghinianus*) and Stephanodiscus (*S. parvus*, *S. hantzschii*) genera. The very high (up to 93%) contribution of oligohalobous diatoms indicated their allochthonous origin from a fluvial environment of the Vistula river. Although planktonic forms dominated the diatom community, 41 out of 55 taxa were benthic, indicating the supply of diatoms washed out from various freshwater habitats. Similar, redeposition and mixing of diatoms from various environments were documented by Razjigaeva et al. (2020) for flood events caused by paleo-typhoons in southern Sakhalin Island.

The diatom assemblages in the studied sediment cores appeared to differ between flood layers interpreted based on the bimodal grain size distribution and in the remaining samples (Figs. 7 and 8). The diatom analyses revealed an increase of up to 30% of oligohalobous halophilus and oligohalobous indifferent taxa associated with a simultaneous decrease in euhalobous and mesohalobous taxa in the flood deposits, which were found to be distinctively different in PCA analysis (Fig. 10). This increase was evident mainly in benthic taxa: *P. brevistriata*, *S. pinnata*, Staurosira (*S. construens*, *S. venter*, *S. binodis*, *S. martyi*, *S. lapponica*), Diploneis (*D. separanda*, *D. elliptica*), Amphora (*A. pediculus*, *A. eximia*, *A. libyca*). It is important to mention that all the benthic diatoms found in the sediment cores were likely redeposited from shallower water depths as the sediment cores were taken from depths below the photic zone. The increased contribution of freshwater diatoms living in different benthic habitats in deposits considered as flood deposits supports the notion of the allochthonous origin of this material delivered by river floods, as suggested by Razjigaeva et al. (2020).

While comparing diatom assemblages structure in flood deposits in cores GC10 and GC11 with the 2010 flood deposits from shallower water depth, there are some differences. The most striking one is the domination of planktic taxa in the flood layer from shallow water sediments. However, one must take into account that the fresh flood deposits were not subjected to mixing with underlying sediments enriched in benthic diatoms. It is also important to note that the river flood also brings benthic diatom assemblages. The flood deposits documented in the sediment cores revealed the increased contribution of the species common in the 2010 flood layer compared to the surrounding sediments. Thus, the composition of the diatoms observed in samples with bimodal grain size distribution may serve as a diagnostic tool in identifying river flood records. However, they also include a taphonomic effect of post-depositional changes (mixing).

5.2. Vistula River flood history

Sedimentary records of floods enable climate and extreme events frequency reconstructions that span well-beyond instrumental time series (Schillereff et al., 2014). Not only were marine records used so far for that purpose, but also lake sediments applying, for instance, variability in sediment magnetic properties (Johansson et al., 2020) and grain size distribution (Chiverrell et al., 2019) as flood proxies. The flood records were also studied in the river valleys (e.g., Starkel et al., 2006; Skolasińska et al., 2015; Reinders, 2022). However, all these records suffer from a lack of completeness, and post-depositional change issues must be addressed (Skolasińska et al., 2015).

Although potentially reflecting large floods of catchment scale and with higher preservation potential, marine sedimentary records are also affected by several critical problems. One of them is related to the fact

that most of the river deltas have many river distributary branches and their relative significance in terms of sediment and water discharge changes in time (e.g., Syvitski et al., 2005). Thus, the river flood sediments may be delivered to the sea from various channels throughout history. The Vistula River also delivered sediment mainly by the western distributary channels near Gdańsk and eastern, entering the Vistula Lagoon (Figs. 1 and 9). The following fundamental issue is the proper study site selection. As supported by the presented observations, the sites that are too shallow (above storm wave base) are not likely to record the finer-grained flood event layers, as the deposits are likely to be reworked and redeposited. On the other hand, the sites located far away from the river mouth may receive too little sediment from the riverine surface plume, and the resulting flood signal may be difficult to identify. It may be the reason for the higher frequency of flood layers found in core GC10 than in GC11, located further away from the river mouth.

The direct correlation of the historical floods (Cyberski, 1995) with the marine sedimentary records is limited for several reasons. The presented cores belong to the best-dated sediment cores from this part of the Baltic Sea so far. However, the uncertainty ranges are still significant and do not allow a clear correlation with particular calendar dates of historical events. It is, in particular, the case of the core GC11. The next problem in such a comparison is related to the often incomplete historical sources, which described major floods affecting upstream cities; such floods could be catastrophic in the river's upper reaches but could be less effective after passing the lower river reaches. Moreover, because river floods may be caused by various factors, sometimes related to quite different climatic conditions, e.g. spring – summer heavy rainfall or late-winter ice-jam, the evidence of flood events does not necessarily lead to straightforward palaeoclimatic conclusions. Finally, several factors affect the final sediment dispersal, including wave climate, seasonal circulation pattern, etc. (e.g., Hill et al., 2007). So in the following, we focus on comparing the higher flood frequency periods, instead of particular single events.

The Vistula River catchment is one of the best-studied in terms of river system development on the Holocene time scale (Starkel et al., 2006) and Macklin et al. (2006) compared it with other well-studied systems in Europe. The Holocene flood records were built applying many ^{14}C dates related mainly to fluvial sediments resulting from river channel changes, as these changes are usually associated with major floods (Starkel et al., 2006; Macklin et al., 2006). These records revealed that during the last five thousand years, the approximated ages of significant floods in the Vistula River basin were: 570, 660, 880, 1040, 1310, 1830, 2810, and 4840 years BP (Macklin et al., 2006). Comparing with the record of bimodal flood layers documented in this work and taking into account the age uncertainties resulting from radiocarbon dating and the approximate dating methodology used by Macklin et al. (2006), we found that there is a general correspondence between the significant flood periods. The major flood layers in the presented here record were dated approximately to 230, 450, 525, 855, 905, 1300, and 1340 years BP in core GC10 and 2835, 3220, 3560, 3590, 3830, and 4390 years BP in core GC11 (Fig. 9). From both, terrestrial and marine records, it is clear that there was a higher frequency of significant flood events in the period of c. 250 to 1350 years BP covering the Medieval Warm Period and the Little Ice Age, thus one of the warmest and coldest periods during the late Holocene. The picture is even more obscure if we focus on the periods of the highest major flood frequencies. In the record based on river valley deposits (Macklin et al., 2006; Starkel et al., 2006), the highest frequency of approximately one major flood every 200 years was noted during the Medieval Warm Period, while in the marine record, the same frequencies (once in 200 years) were documented for the Little Ice Age (in GC10 core) and for the period 2800 to 3800 years BP (in GC11 core). The periods of higher flood frequencies during the Little Ice Age and Medieval Warm Period generally overlap with periods considered as wetter in regional reconstructions based on various sources, like lake level changes, or peatland water table fluctuations (Magny, 2004; Lamentowicz et al., 2008; Gałka et al., 2013; Starkel et al., 2013; Pleskot et al., 2018). Concerning the older stage (2800–3800 years BP), such correspondence is less clear in these reconstructions. However, considering the above stated comments on the sedimentary flood records' limitations, more research is needed to make this flood frequency reconstruction more complete and to relate it to palaeoclimatic conditions. Moreover, the human impact should be considered in the interpretation, at least for the last millennium (e.g., Czerwiński et al., 2022).

5.3. Paleoenvironmental changes

Besides the identification of the flood layers and their analysis on the temporal scale, which were the main objectives of the present work, the analyses provided also new insights into the context of major environmental changes related to climate and anthropogenic impact (Fig. 9). They are mainly evident in variations in grain size as well as in diatom compositions.

5.3.1. Insights from sediment properties

The changes in the mean grain size, as discussed in the previous chapters, reflect the distance from the major source and the effectiveness of sediment redistribution due to waves, currents, etc. Thus, one may expect that the coarsest sediments could be related to major storm events (Moskalewicz et al., 2020; Leszczyńska et al., 2022). Indeed, the coarsest mean grain size was noted in GC10 core (Fig. 9) around the time of the largest documented historical storm in the southern Baltic in the year 1497 CE (Piotrowski et al., 2017). However, the long-term trends need to be analyzed also in the context of sediment supply. For instance, during the period of roughly 550 to 800 years BP, the sand content was the highest in core GC10. This could imply a period of stronger storminess. However, during the same period of time, the main sediment discharge from the Vistula River was likely directed to the Vistula Lagoon (Fig. 9), and thus it could be a reason for the smaller contribution of finer-grained sediments. During the remaining periods covered by the core GC10, the sediment composition was similar and the river mouth was probably nearby Gdańsk.

In the core GC11, covering a longer time scale, a steady increase in the contribution of fine-grained sediments was observed for the last c. 2000 years. This kind of trend may reflect catchment scale change in erosion rate, related to anthropogenic deforestation (Czerwiński et al., 2022) leading to more efficient soil erosion and mobilization of fine-grained fractions. However, such an interpretation needs a more accurate age model in order to assess the potential sediment accumulation changes.

5.3.2. Insights from diatom assemblages

The paleoecological interpretation of the relative abundance of diatoms halobian groups revealed several major stages in both cores. In GC10 three stages were proposed reflecting varied contribution of euhalobous, mesohalobous and oligohalobous groups.

The youngest sediments (from 500 years BP to present) in GC10 were characterized by higher content of oligohalobous diatoms and slightly lower contribution of euhalobous taxa. Among oligohalobous diatoms the most abundantly occurred *Pseudostaurosira brevistriata*, *Staurosira construens*, *Amphora pediculus* and *Staurosirella pinnata* representing freshwater benthic component of the diatom flora with high edaphic preferences. Among euhalobous and mesohalobous taxa decreased contribution of marine benthic diatom *Diploneis bombus* and marine/brackish planktonic *Pseudosolenia calcar-avis* was the most significant while decrease of other marine forms *Actinocyclus octonarius, Thalassiosira oestrupii* and *Thalassiosira levanderi* was less pronounced. *A. octonarius* and *T. levanderi* belong to planktonic species being pollution resistant and considered as component of an “anthropogenic” assemblages (Leśniewska and Witak, 2008). These species have been reported previously also from other parts of the gulf (Witkowski, 1994; Stachura and Witkowski, 1997; Witak et al., 2006). The increasing

contribution of oligohalobous taxa during that stage simultaneously with the higher contribution of eutraphentic taxa could be associated with changes of Vistula River mouth location, decreasing salinity and probably progressive eutrophication of the basin which is in line with previous studies (Leśniewska and Witak, 2008; Szymczak-Żyła et al., 2019).

The second stage recognized in GC10 core, from approximately 1200 to 500 years BP was characterized by higher content of euhalobous diatoms while during the third stage from 1700 to 1200 years BP the increased contribution of mesohalobous diatoms was observed. In contrast to the first stage the contribution of marine taxa *T. oestrupii, T. levanderi* and *D. smithii* increased significantly. Higher contribution of *T. levanderi* indicate that eutrophication was accelerated in the basin already during at that time. The increased contribution of mesohalobous diatoms in the third stage was mostly associated with increased abundance of *P. calcar-avis* and *A. normanii* which is in contrast to earlier studies. According to Witak et al. (2006), *P. calcar-avis* belong to the most characteristic diatoms of the Littorina Sea stage, the older period, while during the Post-Littorina Sea stage was sporadically seen. The differences in the contribution of this species among sampling stations in the Gulf of Gdańsk was, however, observed also earlier (Witkowski, 1994; Witak and Dunder, 2007; Leśniewska and Witak, 2008). A relatively higher abundance of euhalobous and mesohalobous groups during the second and third stages indicated that compared to the first stage the salinity of this part of the Gulf of Gdańsk could be higher.

In the GC11 core, four stages were identified reflecting different contribution of euhalobous, mesohalobous and oligohalobous taxa. In contrast to the GC10 core, the youngest sediments (from 150 years BP to present) were characterized by a higher content of euhalobous diatoms, primarily *Thalassiosira oestrupii* and *T. eccentrica*, representing marine plankton, and the lower contribution of benthic *Diploneis bombus*. The mesohalobous diatoms included mainly *Diploneis didyma*, *Opephora olsenii* and *Nanofrustulum sopotense*. Among oligohalobous diatoms, similarly to GC 10 core the highest abundance was recorded for *Pseudostaurosira brevistriata*, *Staurosirella pinnata*, while *Stephanodiscus parvus*, *Cyclostephanos dubius* and *Stephanocyclus meneghinianus* occured only in the subsurface and flood layers. Occurrence of *S. meneghinianus* and *S. hantzschii* was reported earlier by Stachura and Witkowski (1997) in alluvial sediments reflecting the Vistula River's influence on the study area. Moreover, these species are considered to be pollution-resistant components of diatom assemblages indicating the elevated trophic status of waters.

Diatom flora of the second stage, between 150 and 1300 years BP was relatively similar to the first stage and diatom assemblages found in GC10 core. It was characterized by a higher contribution of oligohalobous diatoms, mainly *S. pinnata*, *P. brevistriata*, *Staurosira binodis*, *S. venter* and *Fragilaria heidenii* var. *istvanffyi*. The euhalobous and mesohalobous taxa *T. oestrupii*, *T. levanderi* and *T. eccentrica* were the most numerous, while *Tryblionella apiculata*, *A. octonarius*, *A. normanii*, *D. bombus*, *D. didyma* and *O. olsenii* occurred less frequently. The third stage, between 1300 and 2800 years BP showed little variability, with a change in the contribution of euhalobous and mesohalobous diatoms. The number of *Actinocyclus normanii*, *A. octonarius*, *D. didyma*, *T. eccentrica*, *T. oestrupii* and *P. calcar-avis* increased. The higher abundance of euhalobous and mesohalobous taxa at that time was most likely correlated with the location of the Vistula and the depth from which the GC11 core was collected (Fig. 1, Table 1) and thus limited supply of river sediments, including redeposited diatoms.

During the fourth stage (2800–4600 BP) the contribution of mesohalobous diatoms was at a fairly stable level, represented by *A. normanii*, *D. didyma*, *Opephora guenter-grassii*, *Pseudostaurosiropsis geocollegarum* and *Stauroforma atomus*. The number of euhalobous species such as *D. bombus*, *Diploneis smithii* increased, while the abundance of *P. calcar-avis* and *T. oestrupii* decreased. The occurrence of *O. guenter-grassi* is in line with earlier studies by Leśniewska and Witak (2008). Its higher abundance also agrees with earlier observations on eutrophication of the basin during that period, documented in biomarkers record (Szymczak-Żyła et al., 2019), however, it could be also related to salinity changes. In contrast to previous studies by Stachura-Suchoples (2006) and Witak (2010), low levels of *Thalassionema nitzschioides* were found in the GC11 core, while *Rhizosolenia hebatata f. hebatata* was not identified at all. Higher contributions of such oligohalobous taxa as *S. pinnata*, *S. binodis*, *P. brevistriata* and *Diploneis oblongella* were found, as mentioned by Witkowski (1994) and Stachura-Suchoples (2006). The presence of these species is also indicative of salinity fluctuations and eutrophic conditions during the Late Littorina Sea stage.

The presented above palaeoenvironmental interpretations must be, however, treated with caution. As noticed before, most of the identified indicative taxa belong to benthic diatoms. However, the sea floor at the coring sites is well beneath the photic zone. Thus, the dominating benthic diatoms are allochthonous, and were transported (and mixed) from shallower environments. It may be, for instance, a reason for the presence of assemblages revealing at the same time taxa typical for higher and lower salinity.

6. Conclusions

The present study of the large flood record of the Vistula River in the Gulf of Gdańsk (Baltic Sea) provided potential tools to identify flood records (bimodal grain size distribution, specific diatom assemblage - elevated amount of planktonic and benthic oligohalobous taxa) in the areas of moderate flood sediment supply. It was found that modern large flood deposits were relatively thin (sub-centimeter), and within a year, they were removed from a water depth of less than 30 m. Thus, the palaeoflood record was searched in sediment cores retrieved from water depths over 60 m, composed mainly of sandy mud. During the last c. 4 ka, a dozen major flood events were identified. However, their application to flood climate reconstruction was difficult because of relatively frequent and partly unknown, changes in major river mouth positions in the past. The present work suggests that thin deposits of major floods left on the seafloor and subjected to further mixing may still be recognized using a combination of detailed grain size analysis with diatom analysis supplemented by a good understanding of the depositional system. It is likely possible to apply this approach not only for the further studies of paleofloods from the Vistula River system but also to other river systems with moderate sediment supply.

Supplementary data to this article can be found online at https://doi.org/10.1016/j.palaeo.2023.111499.

Declaration of Competing Interest

The authors declare that they have no known competing financial interests or personal relationships that could have appeared to influence the work reported in this paper.

Data availability

Data will be made available on request.

Acknowledgements

This study was supported by a grant funded by the Polish National Science Center No. 2013/11/N/ST10/00491, and 'Młodzi Naukowcy' subsidy (2014-2015) from the Adam Mickiewicz University in Poznań. The captain and the crew of R/Y Oceania and the scientific participants of the cruises are acknowledged for their help during the coring. We sincerely thank an anonymous reviewer and the editor Mary Elliot, whose comments helped to improve the manuscript.

References

Anthony, J.E., 2015. Wave influence in the construction, shaping and destruction of river deltas: a review. Mar. Geol. 361, 53–78. https://doi.org/10.1016/j.margeo.2014.12.004.

Bąk, M., Witkowski, A., Żelazna-Wieczorek, J., Szczepocka, E., Szulc, K., Szulc, B., Wojtas, A., 2012. Klucz do oznaczania okrzemek w fitobentosie na potrzeby oceny stanu ekologicznego wód powierzchniowych w Polsce. Biblioteka Monitoringu Środowiska, Główny Inspektorat Ochrony Środowiska, Warszawa, p. 452.

Battarbee, R.W., 1986. Diatom analysis. In: Berglund, B.E. (Ed.), Handbook of Holocene Paleoecology and Paleohydrology. Wiley, London, pp. 527–570.

Bentley, S.J., Nittrouer, C.A., 2003. Emplacement, modification, and preservation of event strata on a flood-dominated continental shelf: Eel shelf, Northern California. Cont. Shelf Res. 23, 1465–1493. https://doi.org/10.1016/j.csr.2003.08.005.

Berner, R., 1984. Sedimentary pyrite formation: An update. Geochim. Cosmochim. Acta 48, 605–615. https://doi.org/10.1016/0016-7037(84)90089-9.

Bertram, H., 1907. Die Entwicklung des Deisch und Entwässerungen im Gebiete des heutigen Daziger Deichverbandes seit dem 14ten Jahrhundert. Danziger Deichamt, Danzig, p. 220.

Bertram, H., Kloeppel, O., La Baume, W., 1924. Das Weischse-Nogat-Delta. In: Beiträge zur Geschichte seiner landschaftlichen Entwicklung, vorgeschichtlichen Besiedlung und bauerlichen Haus- und Hoflannlage. Danziger Verlags-Gesellschaft, Danzing, p. 213.

Blaauw, M., Christen, A., Aquino Lopez, M., Vazquez, J., Gonzalez, O., Belding, T., Theiler, J., Gough, B., Karney, C., 2021. rbacon: Age-Depth Modelling using Bayesian Statistics. https://CRAN.R-project.org/package=rbacon.

Blott, S., Pye, K., 2001. Gradistat: a grain size distribution and statistics package for the analysis of unconsolidated sediments. Earth Surf. Process. Landf. 26, 1237–1248. https://doi.org/10.1002/esp.261.

Börgel, F., Frauen, C., Neumann, T., Schimanke, S., Meier, H.E.M., 2018. Impact of the Atlantic multidecadal oscillation on Baltic Sea variability. Geophys. Res. Lett. 45, 9880–9888. https://doi.org/10.1029/2018GL078943.

Brandstäter, F.A., 1879. Chronologische Uebersicht der Geschichte Danzigs. Verlag von Theodor Bertling, Danzig, p. 114.

Bruel, R., Sabatier, P., 2020. Serac: an R package for ShortlivEd RAdionuclide chronology of recent sediment cores. J. Environ. Radioact. 225, 106449 https://doi.org/10.1016/j.jenvrad.2020.106449.

Bursik, M.I., 1995. Theory of the sedimentation of suspended particles from fluvial plumes. Sedimentology 42, 831–838.

Carlin, J.A., Schreiner, K.M., Dellapenna, T.M., McGuffin, A., Smith, R.W., 2021. Evidence of recent flood deposits within a distal shelf depocenter and implications for terrestrial carbon preservation in non-deltaic shelf settings. Mar. Geol. 431, 106376 https://doi.org/10.1016/j.margeo.2020.106376.

Chiverrell, R.C., Sear, D.A., Warburton, J., Macdonald, N., Schollereff, D.N., Dearing, J. A., Croudace, I.W., Brown, J., Bradley, J., 2019. Using lake sediment archives to improve understanding of flood magnitude and frequency: recent extreme flooding in Northwest UK. Earth Surf. Process. Landf. 44, 2366–2376. https://doi.org/10.1002/esp.4650.

Cieślak, A., Bernat, C., 1969. Dzieje Gdańska. Wydawnictwo Morskie, Gdańsk, p. 570.

Cyberska, B., Krzymiński, W., 1988. Extension of the Vistula River water in the Gulf of Gdansk. In: Proceedings of the. In: 16th Conference of Baltic Oceanographers, Institute of Marine Research, Kiel University, pp. 290–304.

Cyberski, J., 1995. Hydrography of Żuławy Wiślane (Vistula Delta) and its changes over the historical period. J. Coast. Res. Spec. Issue 22, 151–159.

Cyberski, J., Grześ, M., Gutry-Korycka, M., Nachlik, E., Kundzewicz, Z.W., 2006. History of floods on the River Vistula. Hydrol. Sci. J. 51, 799–817. https://doi.org/10.1623/hysj.51.5.799.

Czerwiński, S., Marcisz, K., Wacnik, A., Lamentowicz, M., 2022. Synthesis of palaeoecological data from the Polish Lowlands suggests heterogeneous patterns of old-growth forest loss after the Migration Period. Sci. Rep. 12, 8559. https://doi.org/10.1038/s41598-022-12241-1.

Damrat, M., Zaborska, A., Zajączkowski, M., 2013. Sedimentation from suspension and sediment accumulation rate in the Vistula River prodelta, Gulf of Gdańsk (Baltic Sea). Oceanologia 55, 937–950. https://doi.org/10.5697/oc.55-4.937.

Denys, L., 1991. A check-list of the diatoms in the holocene deposits of the western belgian coastal plain with a survey of their apparent ecological requirements. Introduction, ecological code and complete list. In: Professional Paper Belgische Geologische Dienst, 246, pp. 1–41.

Dippner, J., Voss, M., 2004. Climate reconstruction of the MWP in the Baltic Sea area based on biogeochemical proxies from a sediment record. Baltica 17, 5–16.

Douglas, B.C., 2001. Sea-level change in the era of the recording tide gauge. In: Douglas, B.C., Kearney, M.S., Leatherman, S.P. (Eds.), Sea-level Rise: History and Consequence. Academic Press, San Diego, pp. 37–61. https://doi.org/10.1016/S0074-6142(01)80006-1.

Douglas, B.C., Peltier, W.R., 2002. The puzzle of global sea-level rise. Phys. Today 55, 35–41. https://doi.org/10.1063/1.1472392.

Ducassou, E., Mulder, T., Migeon, S., Gonthier, E., Murat, A., Revel, M., Capotondi, L., Bernasconi, S., Mascle, J., Zaragosi, S., 2008. Nile floods recorded in deep Mediterranean sediments. Quat. Res. 70, 382–391. https://doi.org/10.1016/j.yqres.2008.02.011.

Dura, T., Hemphill-Haley, E., Sawai, Y., Horton, B.P., 2016. The application of diatoms to reconstruct the history of subduction zone earthquakes and tsunamis. Earth Sci. Rev. 152, 181–197. https://doi.org/10.1016/j.earscirev.2015.11.017.

Gałka, M., Miotk-Szpiganowicz, G., Goslar, T., Jęśko, M., van der Knaap, W.O., Lamentowicz, M., 2013. Palaeohydrology, fires and vegetation succession in the southern Baltic during the last 7500 years reconstructed from a raised bog based on multi-proxy data. Palaeogeogr. Palaeoclimatol. Palaeoecol. 370, 209–221. https://doi.org/10.1016/j.palaeo.2012.12.011.

Girguś, R., 2020. Wyjątki ze źródeł historycznych o nadzwyczajnych zjawiskach hydrologicznych i meteorologicznych na ziemiach polskich w latach 1601–1920, Instytut Meteorologii i Gospodarki Wodnej – Państwowy Instytut Badawczy, Warszawa, p. 358.

Goslar, T., Czernik, J., Goslar, E., 2004. Low-energy 14C AMS in Poznań radiocarbon laboratory, Poland. Nucl. Instrum. Methods Phys. Res., Sect. B 223-224, 5–11. https://doi.org/10.1016/j.nimb.2004.04.005.

Grelowski, A., Wojewódzki, T., 1996. The impact of the Vistula River on the hydrological conditions in the Gulf of Gdańsk in 1994. Bull. Sea Fish. Inst. 137, 23–33.

Heaton, T., Köhler, P., Butzin, M., Bard, E., Reimer, R., Austin, W., Bronk Ramsey, C., Grootes, P., Hughen, K., Kromer, B., Reimer, P., Adkins, J., Burke, A., Cook, M., Olsen, J., Skinner, L., 2020. Marine20-the marine radiocarbon age calibration curve (0-55,000 cal BP). Radiocarbon 62, 779–820. https://doi.org/10.1017/RDC.2020.68.

Hill, P.S., Fox, P.S., Crockett, J.S., Curran, K.J., Friedrichs, C.T., Geyer, W.R., Milligan, T. G., Ogston, A.S., Puig, P., Scully, M.E., Traykovski, P.A., Wheatcroft, R.A., 2007. Sediment delivery to the seabed on continental margins. In: Nittrouer, C.A., Austin, J.A., Field, M.E., Kravitz, J.H., Syvitski, J.P.M., Wiberg, P.L. (Eds.), Continental Margin Sedimentation: From Sediment Transport to Sequence Stratigraphy, Special Publication Number 37 of the International Association of Sedimentologists. Blackwell Publishing, Malden, pp. 49–99. https://doi.org/10.1002/9781444304398.ch2.

Hustedt, F., 1939. Die Kieselalgen Deutschlands, Osterreichs und der Schweiz mit Berucksichtigung der ubrigen Lander Europas sowie der angrenzenden Meersgebiete. In: Dr. L. Rabenhorst's Kryptogamen-Flora von Deutschland (Ed.), Osterreich und der Schweiz, Akademische Verlagsgesellschaft Geest und Portig K.-G., Leipzig, vol. 7, Part 3, pp. 557–816.

Jegliński, W., 2013. Rozwój wybrzeża Zatoki Gdańskiej w rejonie ujścia Wisły Martwej. Prz. Geol. 61, 587–595.

Jegliński, W., Uścinowicz, S., Kramarska, R., Przezdziecki, P., 2012. Mapa geologiczna polskich obszarów morskich na potrzeby tzw. dodatkowych warstw wojskowych. Centralne Archiwum Geologiczne PIG-PIB. https://geolog.pgi.gov.pl/#name=53nv8rai9r.

Johansson, F.E., Bakke, J., Støren, E.N., Paasche, Ø., Engeland, K., Arnaud, F., 2020. Lake sediments reveal large variations in flood frequency over the last 6,500 years in South-Western Norway. Front. Earth Sci. 8, 239. https://doi.org/10.3389/feart.2020.00239.

Keen, T.R., Bentley, S.J., Vaughan, W.C., Blain, C.A., 2004. The generation and preservation of multiple hurricane beds in the northern Gulf of Mexico. Mar. Geol. 210, 79–105. https://doi.org/10.1016/j.margeo.2004.05.022.

Kokociński, M., Szczuciński, W., Zgrundo, A., Ibragimow, A., 2009. Diatom assemlages in 26 December 2004 tsunami deposits from coastal zone of Thailand as sediment provenance indicators. Pol. J. Environ. Stud. 18, 93–101.

Kolbe, R.W., 1927. About ecology, morphology and taxonomy of freshwater diatoms. Pflanzenforschung 7, 1–146.

Koszka-Maroń, D., 2009. Facies model of the contemporary delta lobe of the Vistula River. Oceanol. Hydrobiol. Stud. 38 (Sup. 1), 57–68.

Krammer, K., Lange-Bertalot, H., 1986. Bacillarophyceae 2/1. Naviculaceae. In: Ettl, H., Gerloff, J., Heynig, H., Mollenhauser, D. (Eds.), Süsswasserflora von Mitteleuropa. Gustav Fischer Verlag, Stuttgart, pp. 1–876.

Krammer, K., Lange-Bertalot, H., 1988. Bacillarophyceae 2/2. Basillariaceae, Epithemiaceae, Surirellaceae. In: Ettl, H., Gerloff, J., Heynig, H., Mollenhauser, D. (Eds.), Süsswasserflora von Mitteleuropa. Gustav Fischer Verlag, Stuttgart, pp. 1–600.

Krammer, K., Lange-Bertalot, H., 1991a. Bacillarophyceae 2/3. Centrales, Fragilariaceae, Eunotiaceae. In: Ettl, H., Gerloff, J., Heynig, H., Mollenhauser, D. (Eds.), Süsswasserflora von Mitteleuropa. Gustav Fischer Verlag, Stuttgart, pp. 1–600.

Krammer, K., Lange-Bertalot, H., 1991b. Bacillarophyceae 2/4. Achnanthaceae, Kritische Erganzungen zu Navicula (Lineolatae) und Gomphonema. In: Ettl, H. (Ed.), Pascher's Süsswasserflora von Mitteleuropa, vol. 2, part 4. Gustav Fischer Verlag, Stuttgart, pp. 1–437.

Kruk-Dowgiałło, L., Szaniewska, A., 2008. Gulf of Gdańsk and Puck Bay. In: Schiewer, U. (Ed.), Ecology of Baltic Coastal Waters, Ecological Studies, vol. 197. Springer, Berlin, Heidelberg, pp. 139–165. https://doi.org/10.1007/978-3-540-73524-3_7.

Lajczak, A., 2003. Contemporary transport of suspended material and its deposition in the Vistula River, Poland. Hydrobiologia 494, 43–49. https://doi.org/10.1023/A:1025425206799.

Lamentowicz, M., Obremska, M., Mitchell, E.A.D., 2008. Autogenic succession, land-use change, and climatic influences on the Holocene development of a kettle-hole mire in Northern Poland. Rev. Palaeobot. Palynol. 151, 21–40. https://doi.org/10.1016/j.revpalbo.2008.01.009.

Lamentowicz, M., Gałka, M., Lamentowicz, Ł., Obremska, M., Kühl, N., Lücke, A., Jessey, V.E.J., 2015. Reconstructing climate change and ombrotrophic bog development during the last 4000 years in northern Poland using biotic proxies, stable isotopes and trait-based approach. Palaeogeogr. Palaeoclimatol. Palaeoecol. 418, 261–277. https://doi.org/10.1016/j.palaeo.2014.11.015.

Leśniewska, M., Witak, M., 2008. Holocene diatom biostratigraphy of the SW Gulf of Gdańsk, southern Baltic Sea (part III). Oceanol. Hydrobiol. Stud. 37, 35–52. https://doi.org/10.2478/v10009-008-0017-x.

Leśniewska, M., Witak, M., 2011. Diatoms as indicators of eutrophication in the SW part of the Gulf of Gdańsk, the Baltic Sea. Oceanol. Hydrobiol. Stud. 40, 68–81. https://doi.org/10.2478/s13545-011-0008-5.

Leszczyńska, K., Stattegger, K., Moskalewicz, D., Jagodziński, R., Kokociński, M., Niedzielski, P., Szczuciński, W., 2022. Controls on coastal flooding in the southern

Baltic Sea revealed from the late Holocene sedimentary records. Sci. Rep. 12, 9710. https://doi.org/10.1038/s41598-022-13860-4.
Lisimenka, A., Kubicki, A., 2019. Bedload transport in the Vistula River mouth derived from dune migration rates, southern Baltic Sea. Oceanologia 61, 384–394. https://doi.org/10.1016/j.oceano.2019.02.003.
Łomniewski, K., 1960. Ujście Wisły. Rocznik Polskiego Towarzystwa Geologicznego, 29, pp. 391–417.
Łysiak-Pastuszak, E., Drgas, N., Piątkowska, Z., 2004. Eutrophication in the polish coastal zone: the past, present status and future scenarios. Mar. Pollut. Bull. 49, 186–195. https://doi.org/10.1016/j.marpolbul.2004.02.007.
Macklin, M.G., Benito, G., Gregory, K.J., Johnstone, E., Lewin, J., Michczyńska, D.J., Soja, R., Starkel, L., Thorndycraft, V.R., 2006. Past hydrological events reflected in the Holocene fluvial record of Europe. Catena 66, 145–154. https://doi.org/10.1016/j.catena.2005.07.015.
Magny, M., 2004. Holocene climate variability as reflected by mid-European lake-level fluctuations and its probable impact on prehistoric human settlements. Quat. Int. 113, 65–79. https://doi.org/10.1016/S1040-6182(03)00080-6.
Majewski, A., 1994. Natural evironmental conditions of the Gulf of Gdansk and its surroundings. In: Błażejowski, J., Schuller, D. (Eds.), Pollution and Renewal of the Gulf of Gdansk. Gdansk University, Gdańsk, pp. 33–42.
Mathalon, A., Goodman-Tchernov, B., Hill, P., Kálmán, Á., Katz, T., 2019. Factors influencing flashflood deposit preservation in shallow marine sediments of a hyperarid environment. Mar. Geol. 411, 22–35. https://doi.org/10.1016/j.margeo.2019.01.010.
Mendes, I., Lobo, F.J., Hanebuth, T.J.J., López-Quirós, A., Schönfeld, J., Lebreiro, S., Reguera, M.I., Antón, L., Ferreira, Ó., 2020. Temporal variability of flooding events of Guadiana River (Iberian Peninsula) during the middle to late Holocene: Imprints in the shallow-marine sediment record. Palaeogeogr. Palaeoclimatol. Palaeoecol. 556, 109900 https://doi.org/10.1016/j.palaeo.2020.109900.
Milliman, J.D., 1997. Effect of terrestrial processes and human activities on river discharge, and their impact on the coastal zone. In: Haq, B.U., Haq, S.M., Kullenberg, G., Stel, J.H. (Eds.), Coastal Zone Management Imperative for Maritime Developing Nations. Springer, Dordrecht, pp. 75–92.
Milliman, J.D., Syvitski, J.P.M., 1992. Geomorphic/tectonic control of sediment discharge to the ocean: the importance of small mountainous rivers. J. Geol. 100, 525–544. https://doi.org/10.1086/629606.
Miserocchi, S., Langone, L., Tesi, T., 2007. Content and isotopic composition of organic carbon within a flood layer in the Po River prodelta (Adriatic Sea). Cont. Shelf Res. 27, 338–358. https://doi.org/10.1016/j.csr.2005.05.005.
Moskalewicz, D., Szczuciński, W., Mroczek, P., Vaikutiene, G., 2020. Sedimentary record of historical extreme storm surges on the Gulf of Gdańsk coast, Baltic Sea. Mar. Geol. 420, 106084 https://doi.org/10.1016/j.margeo.2019.106084.
Mulder, T., Migeon, S., Savoye, B., Jouanneau, J.M., 2001. Twentieth century floods recorded in the deep Mediterranean sediments. Geology 29, 1011–1014. https://doi.org/10.1130/0091-7613(2001)029<1011:TCFRIT>2.0.CO;2.
Niemkiewicz, E., Wrzołek, L., 1998. Phytoplankton as eutrophication indicators in the Gulf of Gdańsk water. Oceanol. Stud. 27, 77–92.
Nittrouer, C.A., Wright, L.D., 1994. Transport of particles across continental shelves. Rev. Geophys. 32, 85–113. https://doi.org/10.1029/93RG02603.
Nittrouer, C., DeMaster, D.J., McKee, B., Cutshall, N., Larsen, I., 1984. The effect of sediment mixing on Pb-210 accumulation rates for the Washington continental shelf. Mar. Geol. 54, 201–221. https://doi.org/10.1016/0025-3227(84)90038-0.
Ogston, A.S., Cacchione, D.A., Sternbert, R.W., Kineke, G.C., 2000. Observations of storm and river flood driven sediment transport on the northern California continental shelf. Cont. Shelf Res. 20, 2141–2162. https://doi.org/10.1016/S0278-4343(00)00065-0.
Overeem, I., Syvitski, J.P.M., 2009. Dynamics and vulnerability of Delta systems. Land-Ocean Interactions in the coastal zone. In: LOICZ Reports & Studies No. 35. GKSS Research Center, Geesthacht, p. 54.
Pawelec, A., Sapota, M., Kobos, J., 2018. The effect of algal blooms on fish in their inshore nursery grounds in the Gulf of Gdańsk. J. Mar. Biol. Assoc. U. K. 98, 97–104. https://doi.org/10.1017/s0025315417001606.
Piotrowski, A., Szczuciński, W., Sydor, P., Kotrys, B., Rzodkiewicz, M., Krzymińska, J., 2017. Sedimentary evidence of extreme storm surge of tsunami events in the southern Baltic Sea (Rogowo area, NW Poland). Geol. Quart. 61, 973–986. https://doi.org/10.7306/gq.1385.
Pleskot, K., Tjallingii, R., Makohonienko, M., Nowaczyk, N., Szczuciński, W., 2018. Holocene paleohydrological reconstruction of Lake Strzeszyńskie (western Poland) and its implications for the central European climatic transition zone. J. Paleolimnol. 59, 443–459. https://doi.org/10.1007/s10933-017-9999-2.
Pleskot, K., Apolinarska, K., Cwynar, L.C., Kotrys, B., Lamentowicz, M., 2022. The late-Holocene relationship between peatland water table depth and summer temperature in northern Poland. Palaeogeogr. Palaeoclimatol. Palaeoecol. 586, 110758 https://doi.org/10.1016/j.palaeo.2021.110758.
Pliński, M., Mazur-Marzec, H., Jóźwiak, T., Kobos, J., 2007. The potential causes of cyanobacterial blooms in Baltic Sea estuaries. Oceanol. Hydrobiol. Stud. 36, 134–137. https://doi.org/10.2478/v10009-007-0001-x.
Pruszak, Z., van Ninh, P., Szmytkiewicz, M., Manh, Hung N., Ostrowski, R., 2005. Hydrology and morphology of two river mouth regions (temperate Vistula Delta and subtropical Red River Delta). Oceanologia 47, 365–385.
R Core Team, 2021. R: A Language and Environment for Statistical Computing. R Foundation for Statistical Computing, Vienna, Austria. URL. https://www.R-project.org/.
Razjigaeva, N., Ganzey, L., Grebennikova, T., Kornyushenko, T., Ganzei, K.S., Kudryavtseva, E., Prokopets, S., 2020. Environmental changes and human impact on landscapes as recorded in lagoon-lacustrine sequences of Russky Island, South Far East. J. Asian Earth Sci. 197, 104386 https://doi.org/10.1016/j.jseaes.2020.104386.
Reinders, J.B., 2022. Extending flood records of rivers with sediment records. Nat. Rev. Earth Environ. 3, 425. https://doi.org/10.1038/s43017-022-00314-8.
Robbins, J.A., Edgington, D.N., 1975. Determination of recent sedimentation rates in Lake Michigan using Pb-210 and Cs-137. Geochim. Cosmochim. Acta 39, 285–304.
Round, F.E., 1981. The Biology of Algae. Edward Arnold Limited, London, p. 592.
Sakuna, D., Szczuciński, W., Feldens, P., Schwarzer, K., Khokiattiwong, S., 2012. Sedimentary deposits left by the 2004 Indian Ocean tsunami offshore Khao Lak, Andaman Sea (Thailand). Earth Planets Space 64, 931–943. https://doi.org/10.5047/eps.2011.08.010.
Saniewska, D., Bełdowska, M., Bełdowski, J., Jędruch, A., Saniewski, M., Falkowska, L., 2014. Mercury loads into the sea associated with extreme flood. Environ. Pollut. 191, 93–100. https://doi.org/10.1016/j.envpol.2014.04.003.
Schillereff, D., Chiverrell, R., Macdonald, N., Hooke, J., 2014. Flood stratigraphies in lake sediments: a review. Earth Sci. Rev. 135, 17–37. https://doi.org/10.1016/j.earscirev.2014.03.011.
Skolasińska, K., Szczuciński, W., Mitręga, M., Jagodziński, R., Lorenc, S., 2015. Sedimentary record of 2010 and 2011 Warta River seasonal floods in the region of Poznań, Poland. Geol. Quart. 59, 47–60. https://doi.org/10.7306/gq.1179.
Smith, J.E., Bentley, S.J., Snedden, G.A., White, C., 2015. What role do hurricanes play in sediment delivery to subsiding River Deltas? Sci. Rep. 5, 17582. https://doi.org/10.1038/srep17582.
Snoeijs, P., Balashova, N., 1998. Intercalibration and Distribution of Diatom Species in the Baltic Sea, Vol. 5. Opulus Press, Uppsala, p. 127.
Snoeijs, P., Kasperoviciene, J., 1996. Intercalibration and Distribution of Diatom Species in the Baltic Sea, Vol. 4. Opulus Press, Uppsala, p. 126.
Snoeijs, P., Potapova, M., 1993. Intercalibration and Distribution of Diatom Species in the Baltic Sea, Vol. 1. Opulus Press, Uppsala, p. 129.
Snoeijs, P., Potapova, M., 1995. Intercalibration and Distribution of Diatom Species in the Baltic Sea, Vol. 3. Opulus Press, Uppsala, p. 126.
Snoeijs, P., Vilbaste, S., 1994. Intercalibration and Distribution of Diatom Species in the Baltic Sea, Vol. 2. Opulus Press, Uppsala, p. 126.
Sommerfield, C.K., Nittrouer, C.A., 1999. Modern accumulation rates and a sediment budget for the Eel shelf: a flood-dominated depositional environment. Mar. Geol. 154, 227–241. https://doi.org/10.1016/S0025-3227(98)00115-7.
Stachura, K., Witkowski, A., 1997. Response of the Gulf of Gdańsk diatom flora to the sewage run-off from the Vistula river. Fragmenta Floristica Geobotanica 42, 517–545.
Stachura-Suchoples, K., 2006. Diatoms as indicators of the influence of the Vistula River inflow on the Gulf of Gdańsk during the Holocene. In: Ognjanova-Rumenova, N., Manoylov, K. (Eds.), Advances in Phycological Studies, Festschrift in Honour of Prof. Dobrina Temniskova-Topalov. PENSOFT Publishers & University Publishing House, Sofia-Moscow, pp. 283–291.
Starkel, L., Soja, R., Michczyńska, D., 2006. Past hydrological events reflected in Holocene history of polish rivers. Catena 66, 24–33. https://doi.org/10.1016/j.catena.2005.07.008.
Starkel, L., Michczyńska, D., Krąpiec, M., Margielewski, W., Nalepka, D., Pazdur, A., 2013. Progress in the Holocene chrono-climatostratigraphy of polish territory. Geochronometria 40, 1–21. https://doi.org/10.2478/s13386-012-0024-2.
Sternbeck, J., Sohlenius, G., Hallberg, R.O., 2000. Sedimentary trace elements as proxies to depositional changes induced by a Holocene fresh-brackish water transition. Aquat. Geochem. 6, 325–345. https://doi.org/10.1023/A:1009680714930.
Stuiver, M., Reimer, P.J., Reimer, R.W., 2022. CALIB 8.2 [WWW Program]. at. http://calib.org. accessed 2022-05-21.
Sun, D., Bloemendal, J., Rea, D.K., Vandenberghe, J., Jiang, F., An, Z., Su, R., 2002. Grain-size distribution function of polymodal sediments in hydraulic and aeolian environments, and numerical partitioning of the sedimentary components. Sediment. Geol. 152, 263–277. https://doi.org/10.1016/S0037-0738(02)00082-9.
Świątek, M., 2013. Advection of air masses responsible for extreme rainfall totals in Poland, as exemplified by catastrophic floods in Raciborz (July 1997) and Dobczyce (May 2010). Acta Agrophysica 20, 481–494.
Syvitski, J.P.M., Kettner, A.J., Correggiari, A., Nelson, B.W., 2005. Distributary channels and their impact on sediment dispersal. Mar. Geol. 222–223, 75–94. https://doi.org/10.1016/j.margeo.2005.06.030.
Syvitski, J.P.M., Kettner, A.J., Overeem, I., Hutton, E.W.H., Hannon, M.T., Brakenridge, G.R., Day, J., Vörösmarty, C., Saito, Y., Giosan, L., Nicholls, R.J., 2009. Sinking deltas due to human activities. Nat. Geosci. 2, 681–686. https://doi.org/10.1038/ngeo629.
Szczuciński, W., Stattegger, K., Scholten, J., 2009. Modern sediments and sediment accumulation rates on the narrow shelf off Central Vietnam, South China Sea. Geo-Mar. Lett. 29, 47–59. https://doi.org/10.1007/s00367-008-0122-6.
Szczuciński, W., Kokociński, M., Rzeszewski, M., Chagué-Goff, C., Cachao, M., Goto, K., Sugawara, D., 2012. Sediment sources and sedimentation processes od 2011 Tohoku-oki tsunami deposits on the Sendai Plain, Japan - Insight from diatoms, nannoliths and grain size distribution. Sediment. Geol. 282, 40–56. https://doi.org/10.1016/j.sedgeo.2012.07.019.
Szymczak-Żyła, M., Kowalewska, G., 2009. Chloropigments-a in sediments of the Gulf of Gdansk deposited during the last 4000 years as indicators of eutrophication and climate change. Palaeogeogr. Palaeoclimatol. Palaeocol. 284, 283–294. https://doi.org/10.1016/j.palaeo.2009.10.007.
Szymczak-Żyła, M., Krajewska, M., Winogradow, A., Zaborska, A., Breedveld, G.D., Kowalewska, G., 2017. Tracking trends in eutrophication based on pigments in recent coastal sediments. Oceanologia 59, 1–17. https://doi.org/10.1016/j.oceano.2016.08.003.

Szymczak-Żyła, M., Krajewska, M., Witak, M., Ciesielski, T.M., Ardelan, M.V., Jenssen, B. M., Goslar, T., Winogradow, A., Filipkowska, A., Lubecki, L., Zamojska, A., Kowalewska, G., 2019. Present and Past-Millennial Eutrophication in the Gulf of Gdańsk (Southern Baltic Sea). Paleoceanogr. Paleoclimatol. 34, 136–152. https://doi.org/10.1029/2018PA003474.

Traykovski, P., Geyer, W.R., Irish, J.D., Lynch, J.F., 2000. The role of wave-induced density-driven fluid mud flows for cross-shelf transport on the Eel River continental shelf. Cont. Shelf Res. 20, 2113–2140. https://doi.org/10.1016/S0278-4343(00)00071-6.

Uścinowicz, S., 2003. Relative Sea level changes, glacio-isostatis rebound and shoreline displacement in the southern Baltic. In: Polish Geological Institute Special Papiers 10, pp. 5–79.

Uścinowicz, S., 2006. A relative sea-level curve for the Polish Southern Baltic Sea. Quat. Int. 145–146, 86–105. https://doi.org/10.1016/j.quaint.2005.07.007.

Uścinowicz, S., Ebbing, J., Laban, C., Zachowicz, J., 1998. Recent Muds of the Gulf of Gdańsk. Baltica 11, 25–32.

Uścinowicz, S., Zachowicz, J., Miotk-Szpiganowicz, G., Witkowski, A., 2007. Southern Baltic Sea-level oscillations: new radiocarbon, pollen and diatom proof of the Puck Lagoon (Poland). In: Harff, J., Hay, W.W., Tetzlaff, D.M. (Eds.), Coastline Changes: Interrelation of Climate and Geological Processes, The Geological Society of America Special Papers, Vol. 426, pp. 143–158. https://doi.org/10.1130/2007.2426(10).

Uścinowicz, S., Cieślikiewicz, W., Skrzypek, G., Zgrundo, A., Goslar, T., Jędrysek, M.O., Jurys, L., Koszka-Maroń, D., Miotk-Szpiganowicz, G., Sydor, P., Zachowicz, J., 2022. Holocene relative water level and storminess variation recorded in the coastal peat bogs of the Vistula Lagoon, southern Baltic Sea. Quat. Sci. Rev. 296, 107782 https://doi.org/10.1016/j.quascirev.2022.107782.

Van Dam, H., Mertens, A., Sinkeldam, J., 1994. A coded checklist and ecological indicator values of freshwater diatom from the Netherlands. Neth. J. Aquat. Ecol. 28, 117–133. https://doi.org/10.1007/BF02334251.

Voosen, P., 2019. Seas are rising faster than believed at many river deltas. Science 363, 441. https://doi.org/10.1126/science.363.6426.441.

Vos, P.C., de Wolf, H., 1993. Diatoms as a tool for reconstructing sedimentary environments in coastal wetlands; methodological aspects. Hydrobiologia 269 (270), 285–296.

Voss, M., Doppner, J., Humborg, C., Hürdler, J., Korth, F., Neumann, T., Schernewski, G., Venohr, M., 2011. History and scenarios of future development of Baltic Sea eutrophication. Estuar. Coast. Shelf Sci. 92, 307–322. https://doi.org/10.1016/j.ecss.2010.12.037.

Wheatcroft, R.A., Borgeld, J.C., 2000. Oceanic flood deposits on the northern California shelf: large scale distribution and small scale physical properties. Cont. Shelf Res. 20, 2163–2190. https://doi.org/10.1016/S0278-4343(00)00066-2.

Wheatcroft, R.A., Borgeld, J.C., Born, R.S., Drake, D.E., Leithold, E.L., Nittrouer, C.A., Sommerfield, C.K., 1996. The anatomy of an oceanic flood deposits. Oceanography 9, 158–162. https://doi.org/10.5670/oceanog.1996.03.

Wheatcroft, R.A., Sommerfield, C.K., Drake, D.E., Borgeld, J.C., Nittrouer, C.A., 1997. Rapid and widespread dispersal of flood sediment on the northern California margin. Geology 25, 163–166. https://doi.org/10.1130/0091-7613(1997)025<0163:RAWDOF>2.3.CO;2.

Wheatcroft, R.A., Stevens, A., Hunt, L.M., Milligan, T.G., 2006. The large-scale distribution and internal geometry of the fall 2000 Po River flood deposit: evidence from digital X-radiography. Cont. Shelf Res. 26, 499–516. https://doi.org/10.1016/j.csr.2006.01.002.

Witak, M., 2000. A diatom record of late Holocene environmental changes in the Gulf of Gdańsk. Oceanol. Stud. 29, 57–74.

Witak, M., 2010. Application of diatom biofacies in reconstructing the evolution of sedimentary basin. Record from the southern Baltic Sea differentiated by the extent of the Holocene marine transgressions and human impact. In: Diatom Monogr. 12, Gantner, Liechtenstein, p. 295.

Witak, M., 2013a. A review of the diatom research in the Gulf of Gdańsk and Vistula Lagoon (southern Baltic Sea). Oceanol. Hydrobiol. Stud. 42, 336–346. https://doi.org/10.2478/s13545-013-0091-x.

Witak, M., 2013b. Diatom biofacies in the SW Gulf of Gdańsk and the Vistula Lagoon (the southern Baltic Sea) as indicators of the basin evolution in the Middle and late Holocene. Oceanol. Hydrobiol. Stud. 42, 70–88. https://doi.org/10.2478/s13545-013-0052-4.

Witak, M., Dunder, J., 2007. Holocene diatom biostratigraphy of the SW Gulf of Gdańsk, Southern Baltic Sea (part II). Oceanol. Hydrobiol. Stud. 36, 3–20.

Witak, M., Pędziński, J., 2018. Diatom record of progressive anthropopressure in the Gulf of Gdańsk and the Vistula Lagoon. Oceanol. Hydrobiol. Stud. 47, 167–180. https://doi.org/10.1515/ohs-2018-0016.

Witak, M., Jankowska, D., Piekarek-Jankowska, H., 2006. Holocene diatom biostratigraphy of the southwestern Gulf of Gdańsk, Southern Baltic Sea (Part I). Oceanol. Hydrobiol. Stud. 35, 307–329.

Witkowski, A., 1994. Recent and fossil diatom flora of the Gulf of Gdańsk, Southern Baltic Sea. Bibl. Diatomol. 28, 313.

Witkowski, A., Lange-Bertalot, H., Metzeltin, D., 2000. Diatom flora of marine coasts. In: Iconongraphia Diatomologica, 7. A.R.G. Gantner Verlag K.G., Ruggell, p. 950.

Woszczyk, M., Bechtel, A., Püttmann, W., Rzodkiewicz, M., 2021. Effects of environmental history and post-depositional processes on the organic matter record of Lake Łebsko, Poland. Org. Geochem. 155, 104209 https://doi.org/10.1016/j.orggeochem.2021.104209.

Wróblewski, R., Rudowski, S., Gajewski, Ł., Sitkiewicz, P., Szefler, K., Kałas, M., Koszałka, J., 2015. Changes of the Vistula River External Delta in the period of 2009-2014. Bull. Maritime Inst. Gdańsk 30, 16–22. https://depot.ceon.pl/handle/123456789/8311.

Zajączkowski, M., Darecki, M., Szczuciński, W., 2010. Report on the development of the Vistula river plume in the coastal waters of the Gulf of Gdańsk during the May 2010 flood. Oceanologia 52, 311–317. https://doi.org/10.5697/oc.52-2.311.